UNION POUR LA SCIENCE ET LA TECHNOLOGIE VERRIÈRES

USTV SCHOOL ON THE CHARACTERIZATION OF GLASS STRUCTURE

How to assess the glass structure

November 18-22, 2019

POLYTECH ORLÉANS

UNIVERSITE D'ORLEANS

Cemhti

cnrs

Contribution of infrared spectroscopy to the analysis of the glass structure

Domingos De Sousa Meneses

CEMHTI UPR3079 CNRS, Univ. Orléans, F-45071 Orléans, France

e-mail: desousa@cnrs-orleans.fr

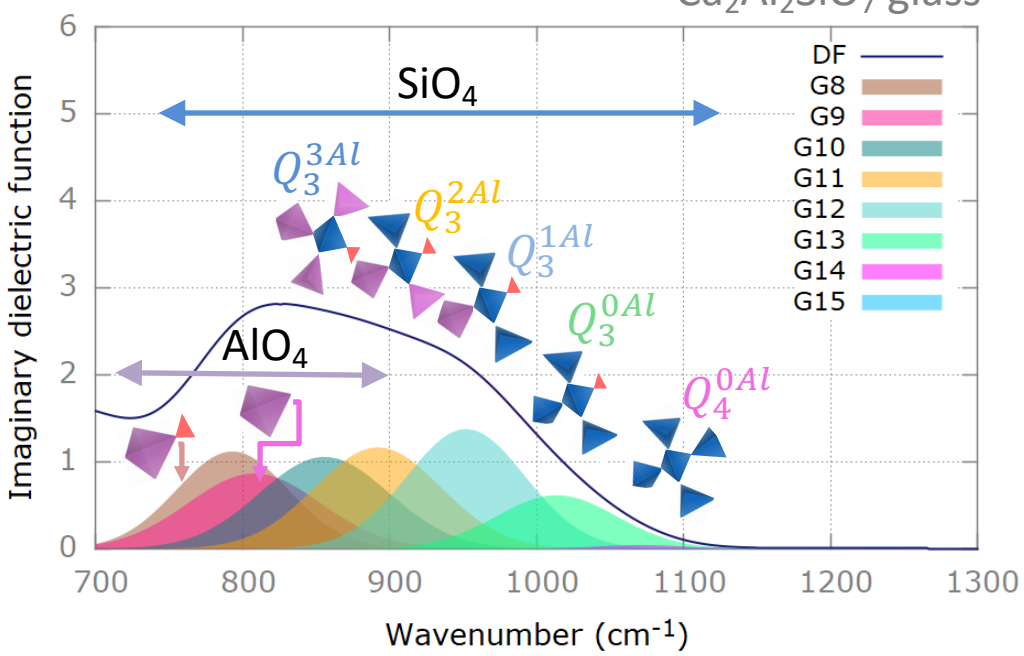

Q_n^{mAl} structural units

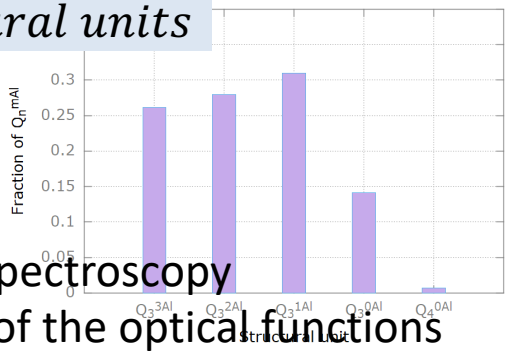

- Infrared spectroscopy
- Retrieval of the optical functions
- Dielectric function models
- Focus software
- Origin of the vibrational modes
- Silicates glasses
- Aluminosilicate glasses
- Iron in silicate glasses and melts

Infrared spectroscopy

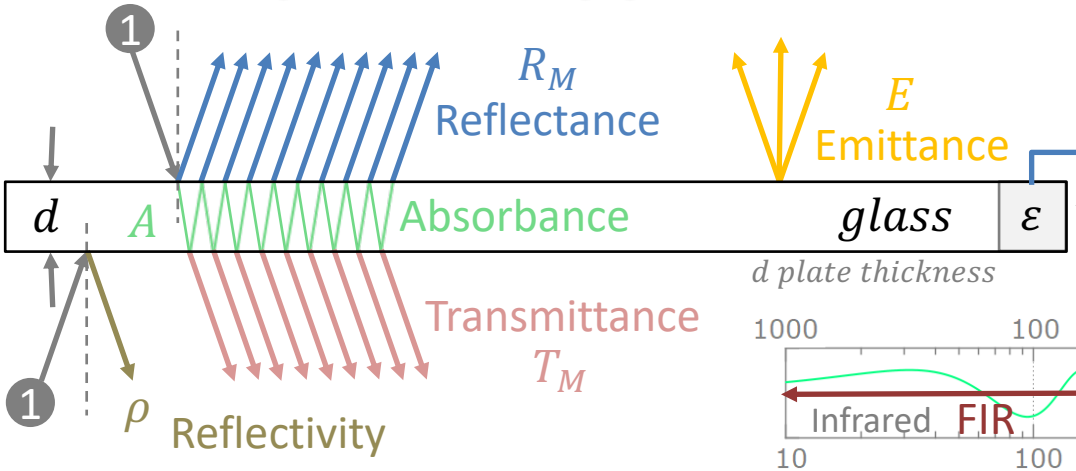

$\varepsilon = \varepsilon' + i\,\varepsilon''$ *dielectric function*

$N = \sqrt{\varepsilon} = n + i\,k$ *complex refractive index*

$\tau = exp(-4\pi k \varpi d)$ *attenuation factor*

d plate thickness

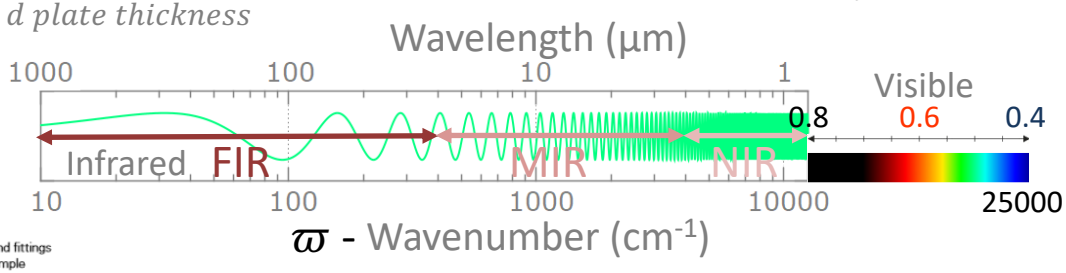

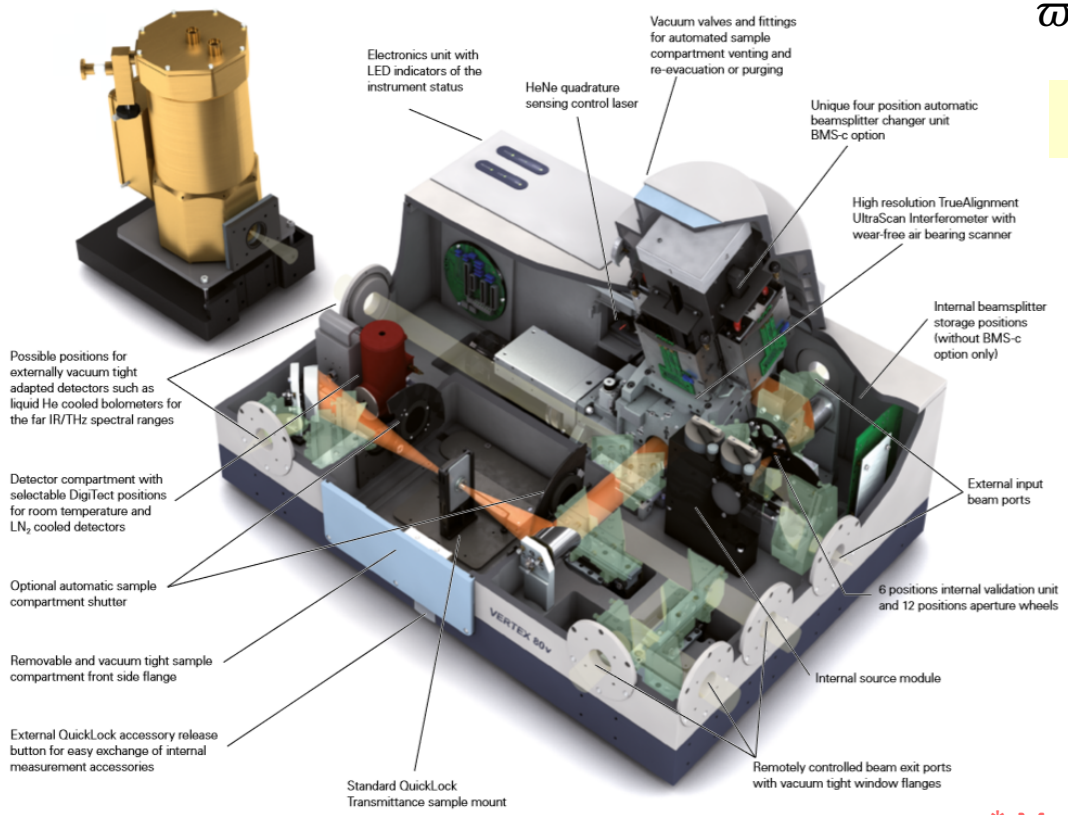

Experimental observables *

Parallel plate sufficiently thick to avoid the observation of interferences

Reflectivity $\rho = \dfrac{(n-1)^2 + k^2}{(n+1)^2 + k^2}$

Reflectance $R_M = \rho\left[1 + \dfrac{(1-\rho)^2\tau^2}{1-\rho^2\tau^2}\right]$

Transmittance $T_M = \tau\dfrac{1-\rho}{1+\rho}\dfrac{1-\rho^2}{1-\rho^2\tau^2}$

Absorbance and Emittance

$$E = A = 1 - R_M - T_M = \frac{(1-\rho)(1-\tau)}{1-\rho\tau}$$

* Measurement at near-normal incidence

Emittance measurement

$L_{BB}(\varpi, \hat{T})$ $L(\varpi, \hat{T}, \theta)$

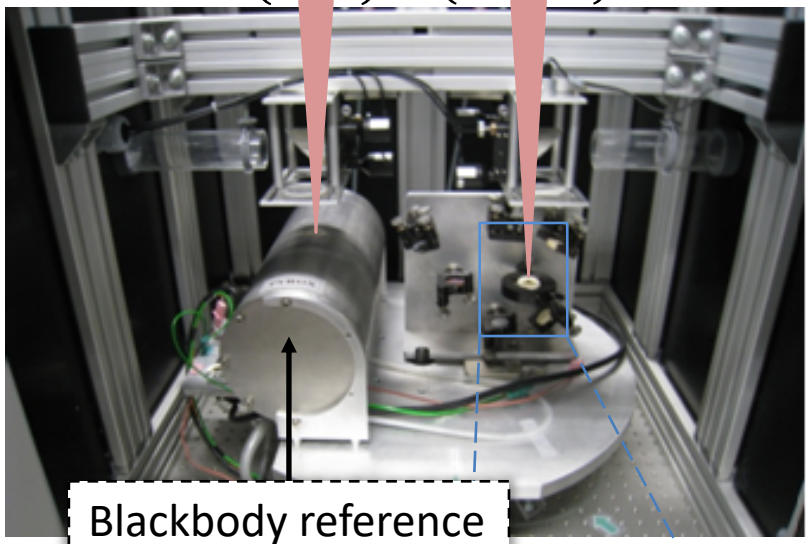

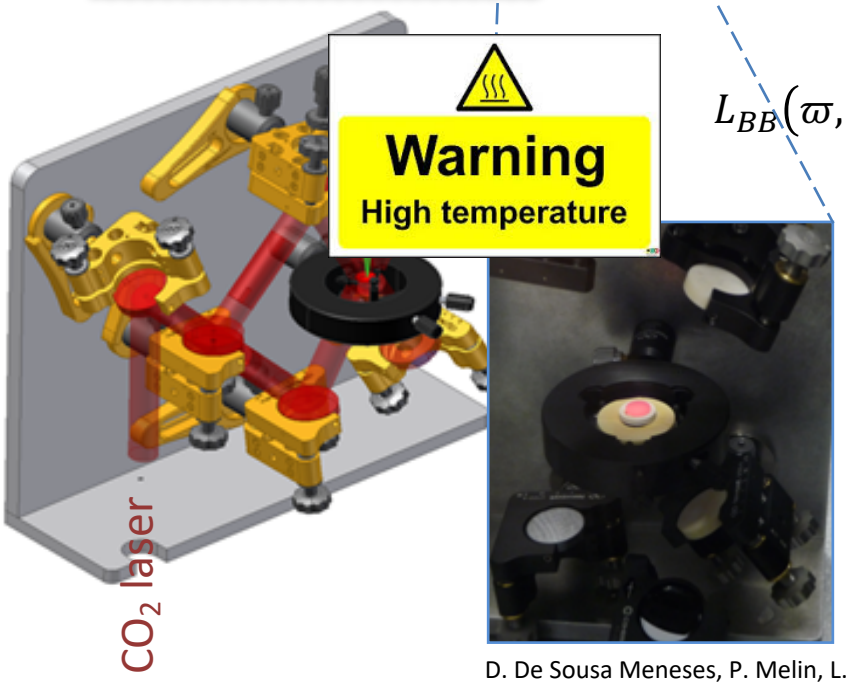

Directional spectral emittance measurement

Ratio of the intensities emitted by the sample and a blackbody in the same conditions

$$E(\varpi, \hat{T}, \theta) = \frac{L(\varpi, \hat{T}, \theta)}{L_{BB}(\varpi, \hat{T})}$$

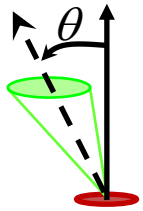

$\hat{T}$: *temperature*

Blackbody

Ideal radiator whose spectral intensity is given by the Planck's law

$$L_{BB}(\varpi, \hat{T}) = \frac{C_1 \varpi^3}{exp\left(\frac{C_2 \varpi}{\hat{T}}\right) - 1}$$

$C_1 = 1{,}191043\ 10^{-16}\ \mathrm{W}.m^2.Sr^{-1}$

$C_2 = 0{,}01438777\ \mathrm{mK}$

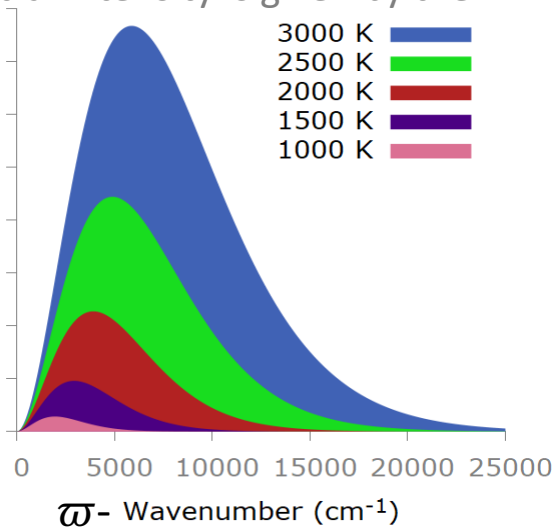

Kirchhoff's law

At LTE, spectral absorptance A and emittance are equal

$$A(\varpi) = E(\varpi)$$

D. De Sousa Meneses, P. Melin, L. del Campo, L. Cosson, P. Echegut Infrared Physics & Technology 69 96–101 2015

Infrared emission spectrometer

Bruker Vertex 80v and Vertex 70

Spectral range : [20-20 000 cm^{-1}](500-0.5 µm)

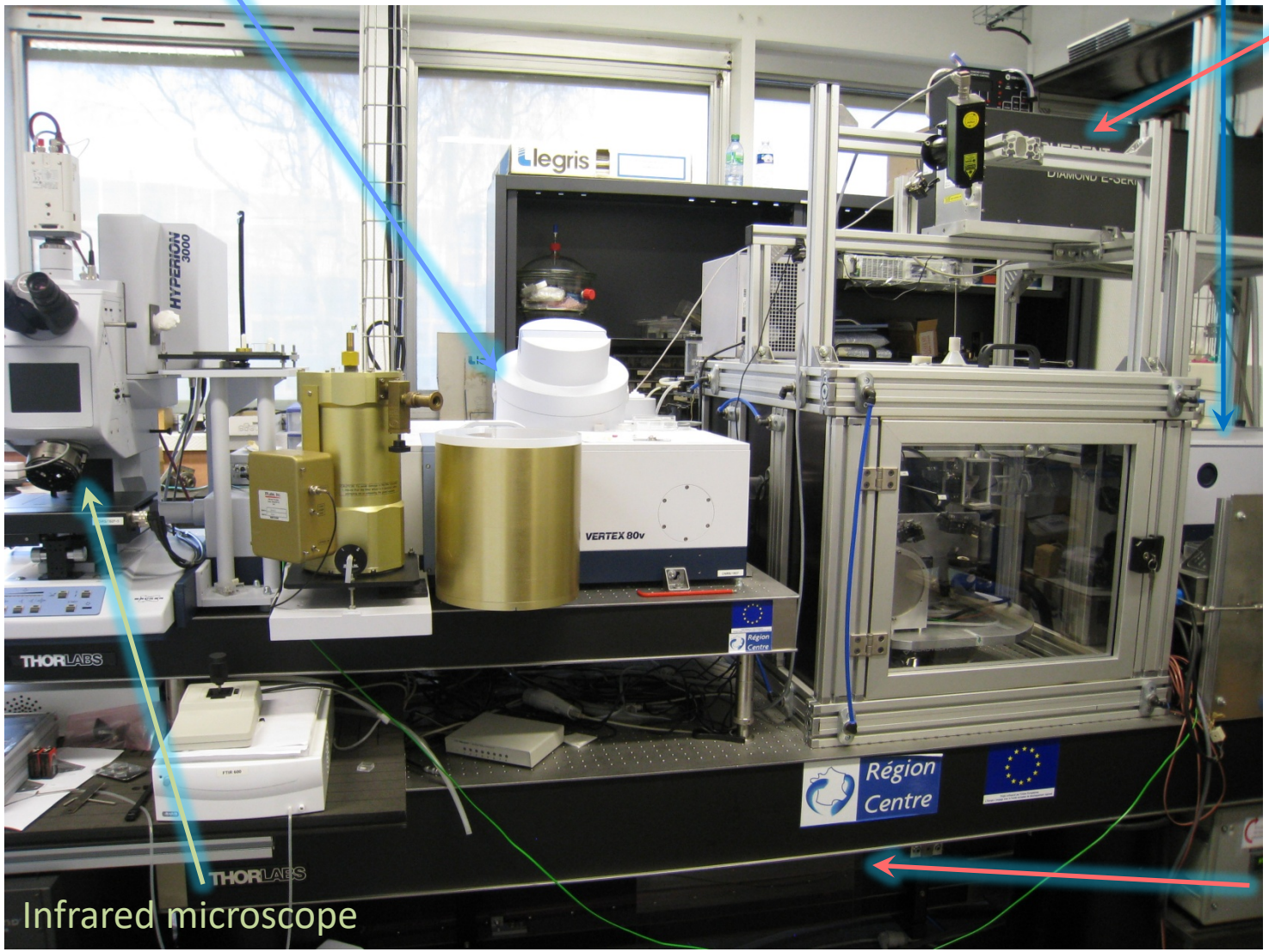

CO_2 laser (500W)
[400 - 3000 K]

Measurements
Reflection R
Transmission T

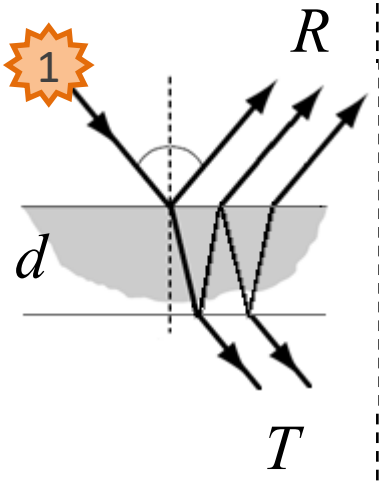

Emission E

CO_2 laser (500W)
[400 - 3000 K]

D. De Sousa Meneses, P. Melin, L. del Campo, L. Cosson, P. Echegut Infrared Physics & Technology 69 96–101 2015

Infrared spectroscopy

SiO_2

Reflectivity - ρ

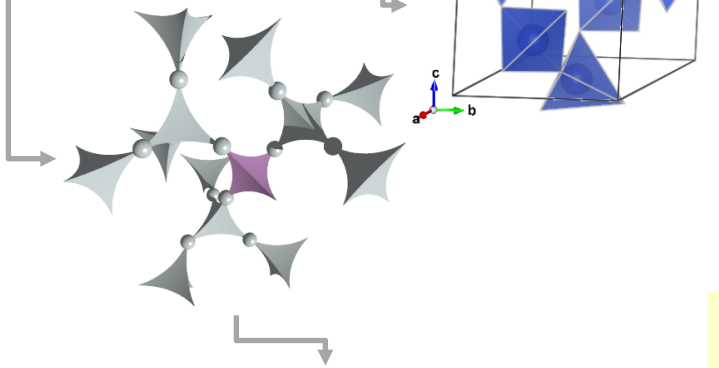

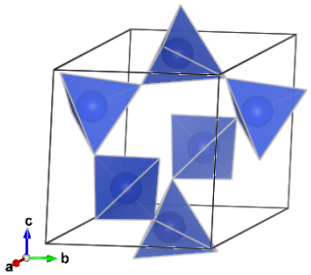

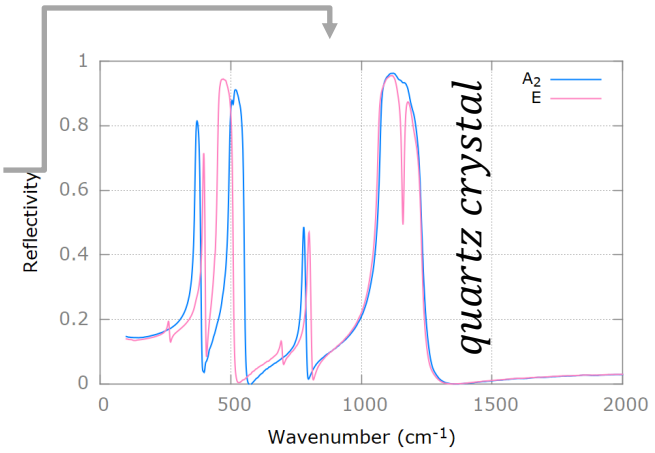

Single crystal

Anisotropic infrared response.

Activity of normal modes (phonons) fixed by crystal symmetry and infrared spectroscopy selection rules

From experimental observables to physical properties

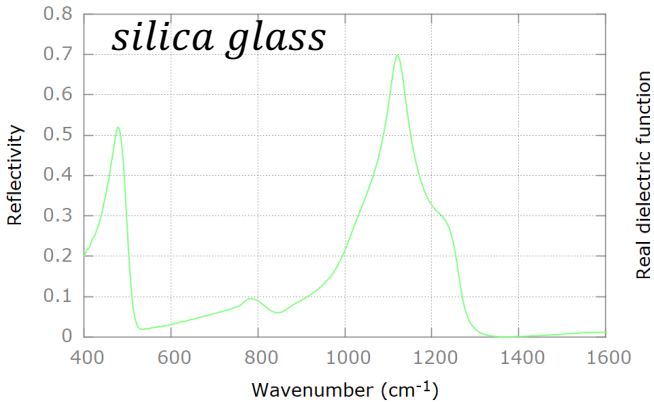

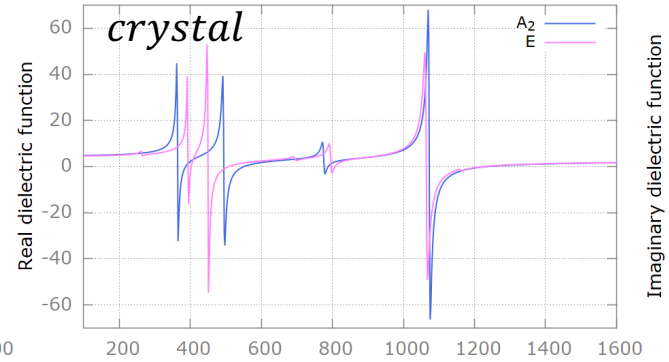

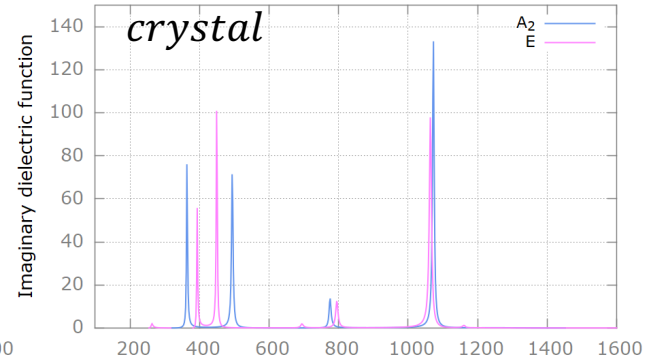

Glass

Isotropic infrared response.

The complexity of the glass structure is revealed by its polar vibrational dynamics.

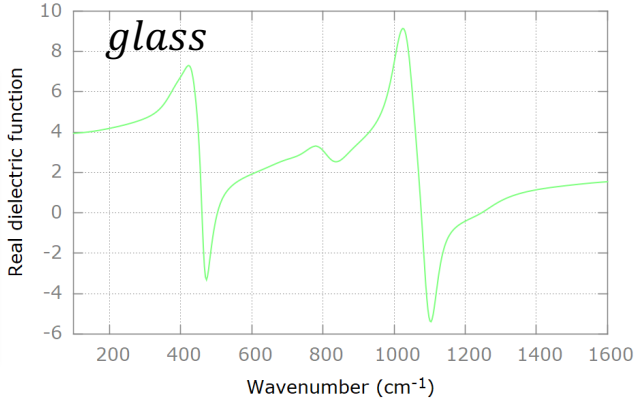

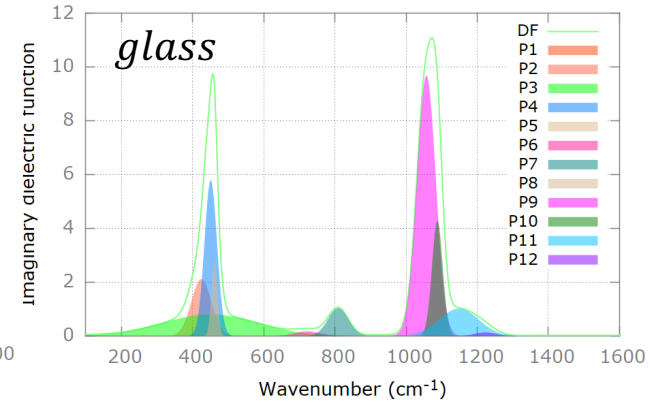

Complex refractive index extraction – inversion methods

IR-Visible-UV spectroscopies Ellipsometry

	R_p	R_s	ρ	R_M	T_M	E	ψ	Δ
R_p								
R_s								
ρ								
R_M								
T_M								
E								
ψ								
Δ								

Several inversion methods necessitates the knowledge of two experimental quantities.

Under certain conditions, 1 measure may be sufficient to determine the indices

Semi-transparent media

R_M T_M | R_M E | T_M=1-R_M-E | T_M E | R_M=1-T_M-E

$$\rho = \frac{R_M(R_M-2) - T_M^2 - 1 + \sqrt{[1+T_M^2 - R_M(R_M-2)]^2 + 4R_M(R_M-2)}}{2(R_M-2)}$$

$$\tau = \frac{1}{T_M}\left(\frac{R_M}{\rho} - 1\right)$$

$$n(\varpi) = \frac{1+\rho(\varpi) + \sqrt{4\rho(\varpi) - (\rho(\varpi)-1)^2 k(\varpi)^2}}{1-\rho(\varpi)}$$

$$k(\varpi) = -\frac{ln(\tau(\varpi))}{4\pi\varpi d}$$

Semi-infinite media

ψ,Δ

$$n(\varpi) + ik(\varpi) = sin(\theta_0)\sqrt{1 + \left[\frac{1+tan(\Psi(\varpi))e^{i\Delta(\varpi)}}{1-tan(\Psi(\varpi))e^{i\Delta(\varpi)}}\right]^2 tan^2(\theta_0)}$$

θ_0 : angle of incidence

KK Inversion method using the Kramers-Kronig relations

$$\delta(\varpi_a) = \frac{1}{2\pi}\int_0^\infty ln\left|\frac{\varpi-\varpi_a}{\varpi+\varpi_a}\right| \frac{d}{d\varpi} ln[\rho(\varpi)]\, d\varpi \qquad n(\varpi) = \frac{1-\rho(\varpi)}{1+\rho(\varpi) - 2\sqrt{\rho(\varpi)}\cdot cos[\delta(\varpi)]} \qquad k(\varpi) = \frac{2\sqrt{\rho(\varpi)}\cdot sin[\delta(\varpi)]}{1+\rho(\varpi) - 2\sqrt{\rho(\varpi)}\cdot cos[\delta(\varpi)]}$$

D. De Sousa Meneses, J-F. Brun, P. Echegut, P. Simon Applied Spectroscopy 58 (2004) 969-974
Kramers-Kronig Relations in Optical Materials Research, Lucarini, V., Saarinen, J.J., Peiponen, K.-E., Vartiainen, E.M. Springer Series in Optical Sciences, Vol. 110 (2005)

Complex refractive index extraction – inversion methods

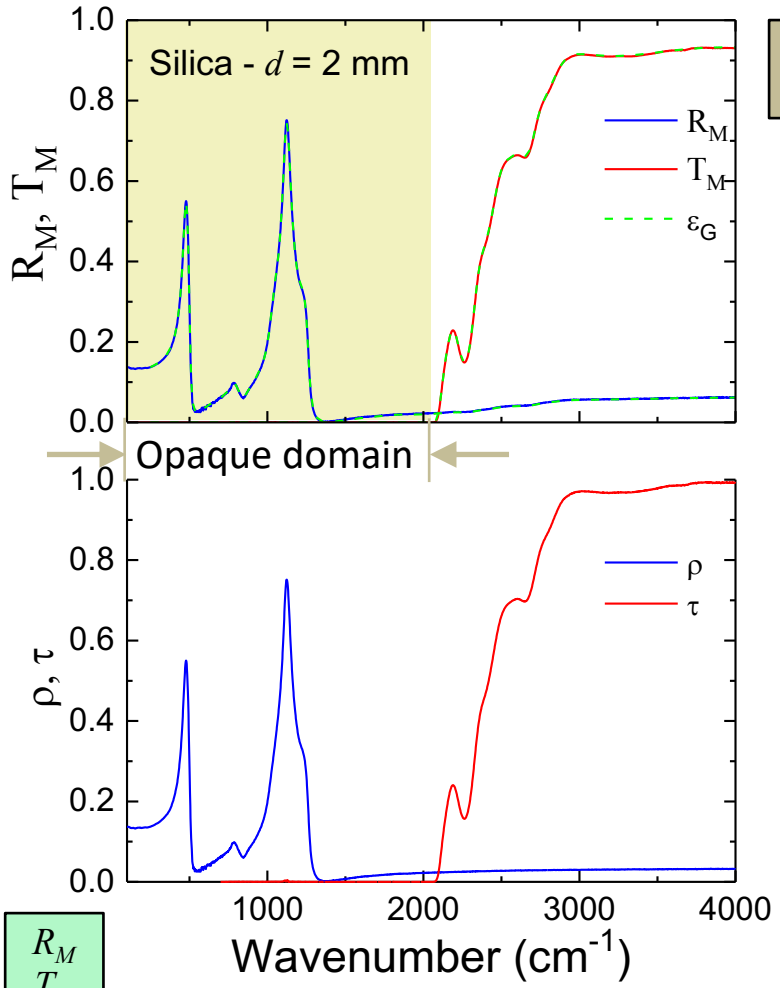

R_M T_M

$$\rho = \frac{R_M(R_M-2) - T_M^2 - 1 + \sqrt{[1+T_M^2 - R_M(R_M-2)]^2 + 4R_M(R_M-2)}}{2(R_M-2)}$$

$$\tau = \frac{1}{T_M}\left(\frac{R_M}{\rho} - 1\right)$$

$$n(\varpi) = \frac{1+\rho(\varpi) + \sqrt{4\rho(\varpi) - (\rho(\varpi)-1)^2 k(\varpi)^2}}{1-\rho(\varpi)} \qquad k(\varpi) = -\frac{ln(\tau(\varpi))}{4\pi\varpi d}$$

KK

$$\delta(\varpi_a) = \frac{1}{2\pi}\int_0^\infty ln\left|\frac{\varpi-\varpi_a}{\varpi+\varpi_a}\right| \frac{d}{d\varpi} ln[\rho(\varpi)]\, d\varpi$$

$$n(\varpi) = \frac{1-\rho(\varpi)}{1+\rho(\varpi) - 2\sqrt{\rho(\varpi)}\cdot cos[\delta(\varpi)]} \qquad k(\varpi) = \frac{2\sqrt{\rho(\varpi)}\cdot sin[\delta(\varpi)]}{1+\rho(\varpi) - 2\sqrt{\rho(\varpi)}\cdot cos[\delta(\varpi)]}$$

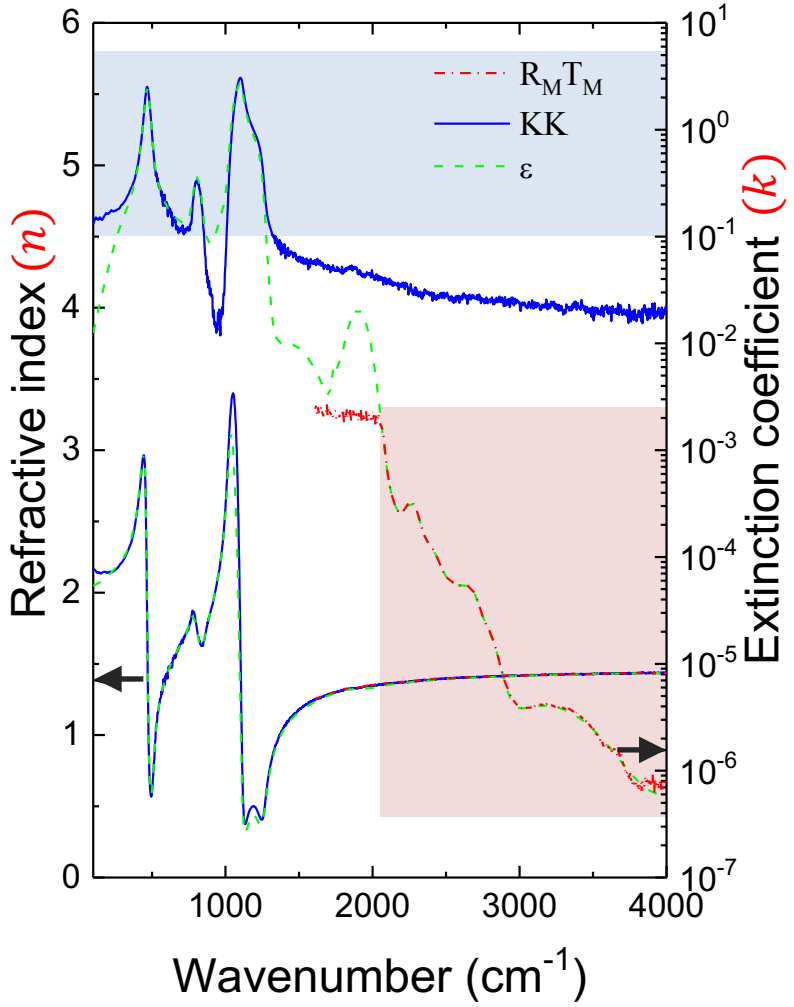

Dielectric function models – disordered media

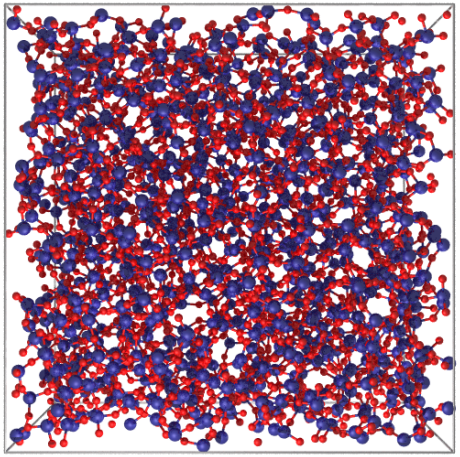

Lorentz model

Single crystals

$$\varepsilon(\varpi) = \varepsilon_\infty + \sum_j \frac{S_j \varpi_j^2}{\varpi_j^2 - \omega^2 - i\gamma_j \varpi}$$

The Lorentz dielectric function model (DHO - Damped Harmonic Oscillator) used for the adjustment of crystal spectra is not suitable for glasses.

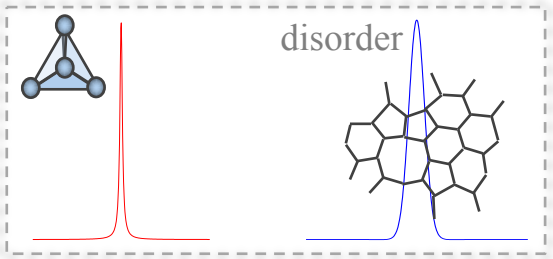

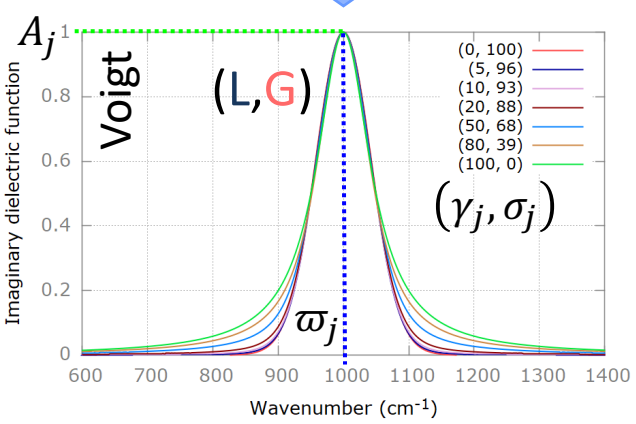

Causal Voigt model

Allows to account for a Gaussian (G) broadening of a Lorentzian absorption profile (L).

$$\varepsilon_V(\varpi) = \varepsilon_\infty + \sum_j \hat{V}_j(\varpi) = \varepsilon_\infty + \sum_j \hat{V}\left(\varpi; A_j, \varpi_j, \gamma_j, \sigma_j\right)$$

$$\hat{V}_j(\varpi) = \hat{V}_j(x,y) = A_j \left[-\frac{\Im\left(w(x - x_j + iy) + w(x + x_j + iy)\right)}{\Re\left(w(iy)\right)} + i\frac{\Re\left(w(x - x_j + iy) - w(x + x_j + iy)\right)}{\Re\left(w(iy)\right)} \right]$$

$$x = \frac{2\sqrt{\ln 2}}{\sigma_j}\varpi \qquad x_j = \frac{2\sqrt{\ln 2}}{\sigma_j}\varpi_j \qquad y = \frac{\gamma_j}{\sigma_j}\sqrt{\ln 2}$$

Faddeeva function: $w(z) = \frac{i}{\pi}\int_{-\infty}^{+\infty} \frac{e^{-t^2}}{z - t} dt = K(x,y) + i\,J(x,y)$

D. De Sousa Meneses et al. J. Non-Cryst. Solids 351 (2005) 124-129.

Dielectric function models – disordered media

Convolution model

Expression based on a Gaussian distribution of damped harmonic oscillators

$$\varepsilon(\varpi) = \varepsilon_\infty + \sum_j \frac{S_j}{\sqrt{2\pi}\sigma_j} \int_{-\infty}^{+\infty} \frac{exp\left[-\frac{1}{2}\left(\frac{x-\varpi_j}{\sigma_j}\right)^2\right]}{x^2 - \varpi^2 - i\gamma_j\varpi} dx$$

H. Hobert, H. H. Dunken J. Non-Cryst. Solids 195 (1996) 64-71
A. M. Efimov, J. Non-Cryst. Solids 203 (1996) 1.
T. G. Mayerhofer et al. J. Non-Cryst. Solids 333 (2004) 172–181.

The Voigt and convolution models have close absorption profiles for high frequency modes with low inhomogeneous broadening. The difference can be large at low frequency.

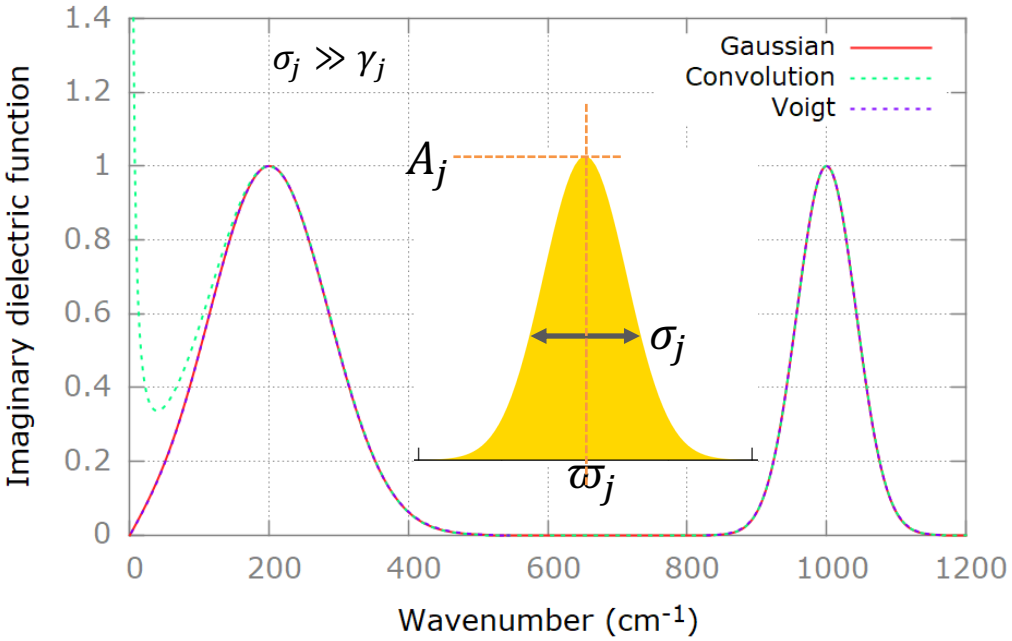

Causal Gaussian model

Allows to take into account several components having a Gaussian absorption profile respecting the causality principle.

$$\varepsilon(\varpi) = \varepsilon_\infty + \sum_j \frac{2A_j}{\sqrt{\pi}} \left[D\left(2\sqrt{ln2}\,\frac{\varpi+\varpi_j}{\sigma_j}\right) - D\left(2\sqrt{ln2}\,\frac{\varpi-\varpi_j}{\sigma_j}\right)\right] + i\,A_j\left[exp\left(-4ln2\left(\frac{\varpi-\varpi_j}{\sigma_j}\right)^2\right) - exp\left(-4ln2\left(\frac{\varpi+\varpi_j}{\sigma_j}\right)^2\right)\right]$$

Dawson function: $D(x) = \exp(-x^2)\int_0^x \exp(t^2)\,dt$

D. De Sousa Meneses, M. Malki, P. Echegut, J. Non-Cryst. Solids 351 (2006) 769-776.

Normal spectral emittance of a silica glass

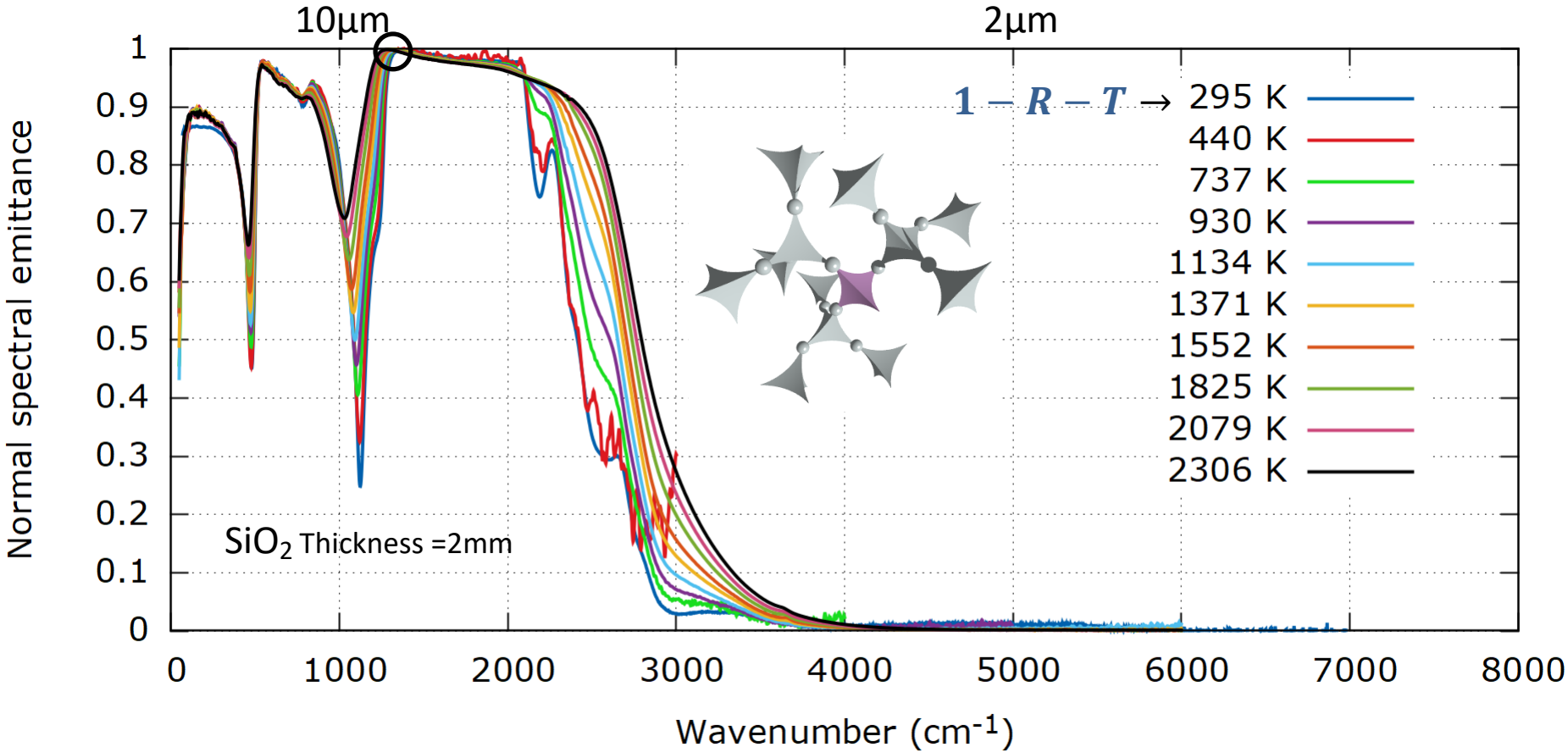

Temperature measurement at the Christiansen point ○ $n = 1, k \ll 1 \rightarrow E \cong 1$

Retrieval of the complex refractive index $N(\varpi) = n(\varpi) + i\,k(\varpi)$

Fit of the data with the following parallel plate model of emittance (E):

$$E = \frac{(1-\rho)(1-\tau)}{1-\rho\tau} \qquad \rho = \frac{(n-1)^2 + k^2}{(n+1)^2 + k^2} \qquad \tau = exp(-4\pi k \varpi d)$$

d : sample thickness

Fit with a dielectric function model

Dielectric function : $\varepsilon(\varpi) = [N(\varpi)]^2$

Causal Gaussian dielectric function model for glasses

$$\varepsilon(\varpi) = \varepsilon_\infty + \sum_j \frac{2A_j}{\sqrt{\pi}} \left[D\left(2\sqrt{ln2}\,\frac{\varpi+\varpi_j}{\sigma_j}\right) - D\left(2\sqrt{ln2}\,\frac{\varpi-\varpi_j}{\sigma_j}\right) \right] + i\,A_j \left[exp\left(-4ln2\left(\frac{\varpi-\varpi_j}{\sigma_j}\right)^2\right) - exp\left(-4ln2\left(\frac{\varpi+\varpi_j}{\sigma_j}\right)^2\right) \right]$$

D is the Dawson function

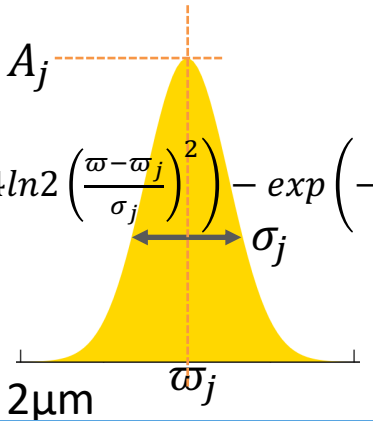

Examples of fit of emittance spectra of a silica glass

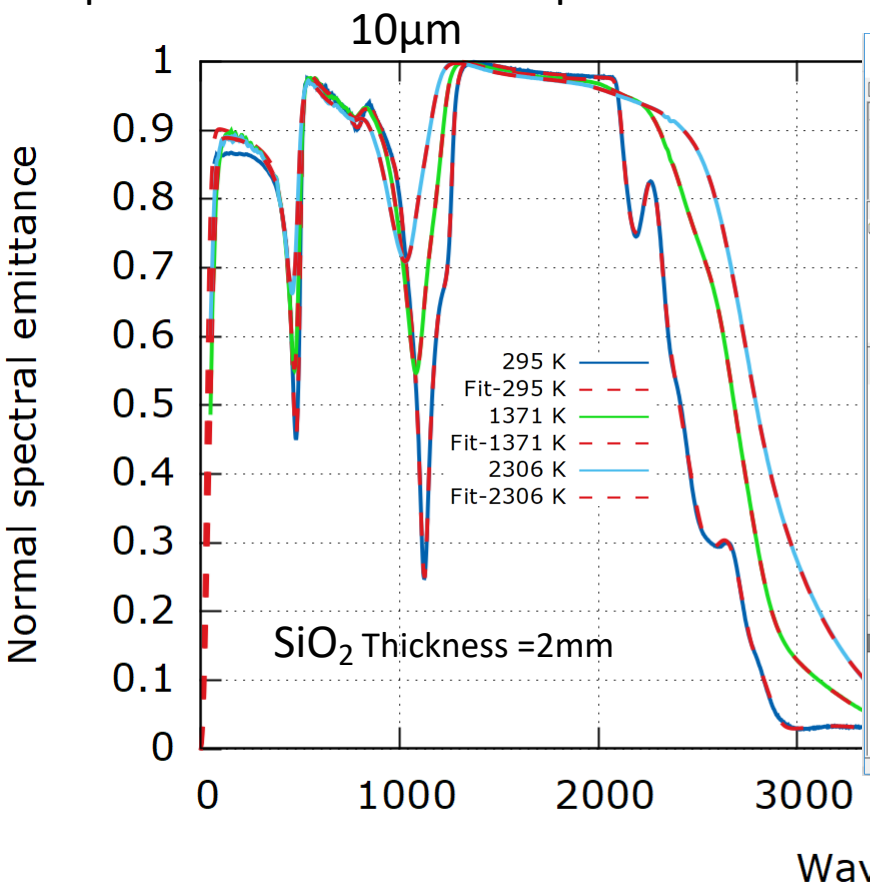

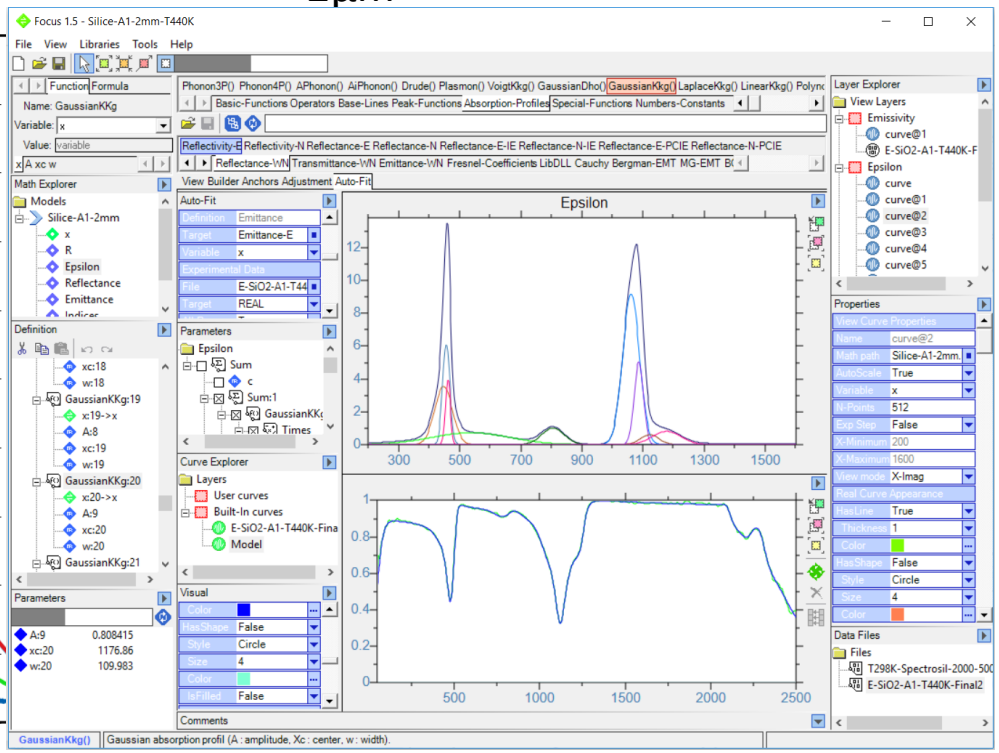

Complex refractive index of the silica sample

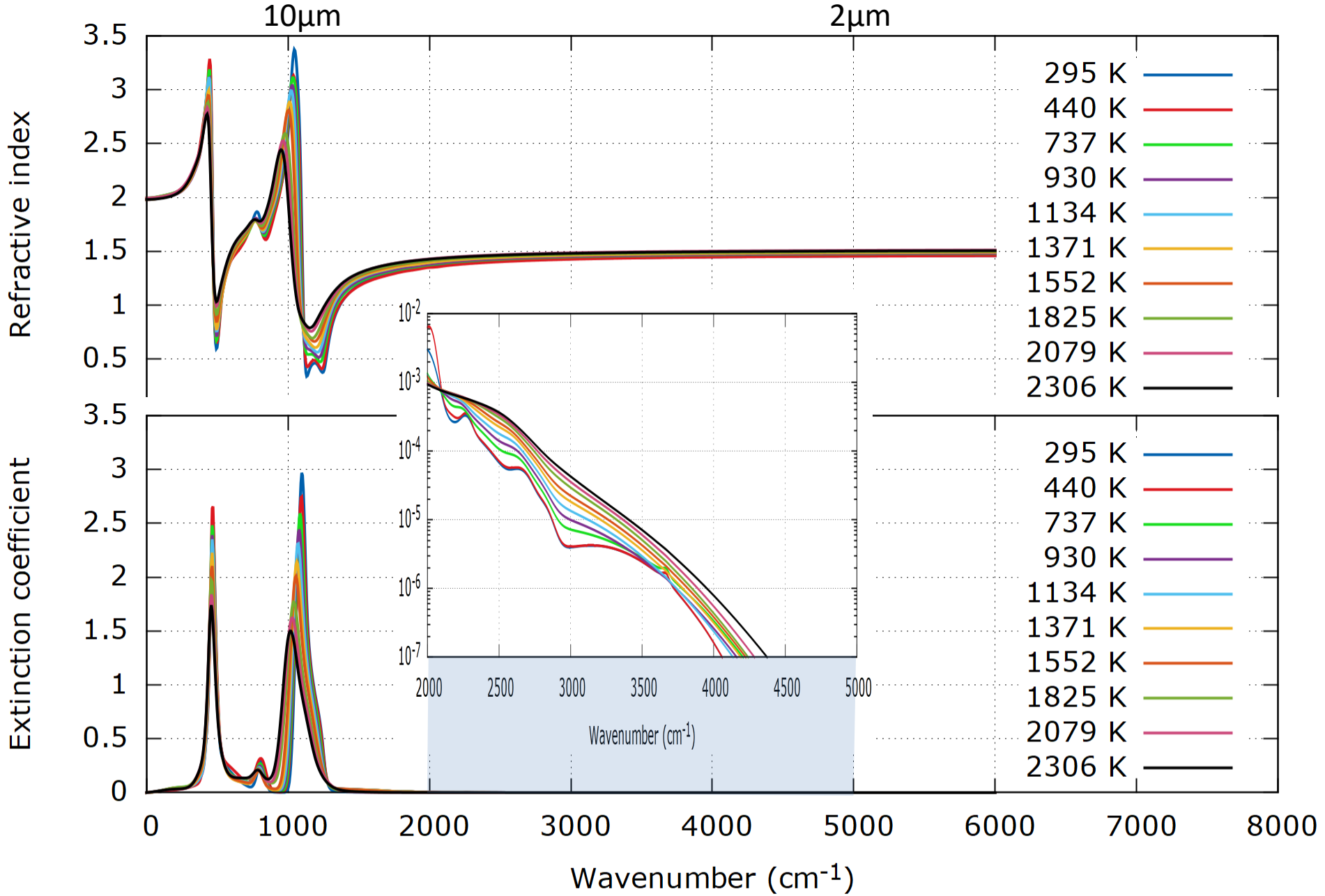

Fit of the reflectivity of a glass with different models

Lorentz model

Gaussian model

$(CaO)_x(P_2O_5)_{1-x}$ glass

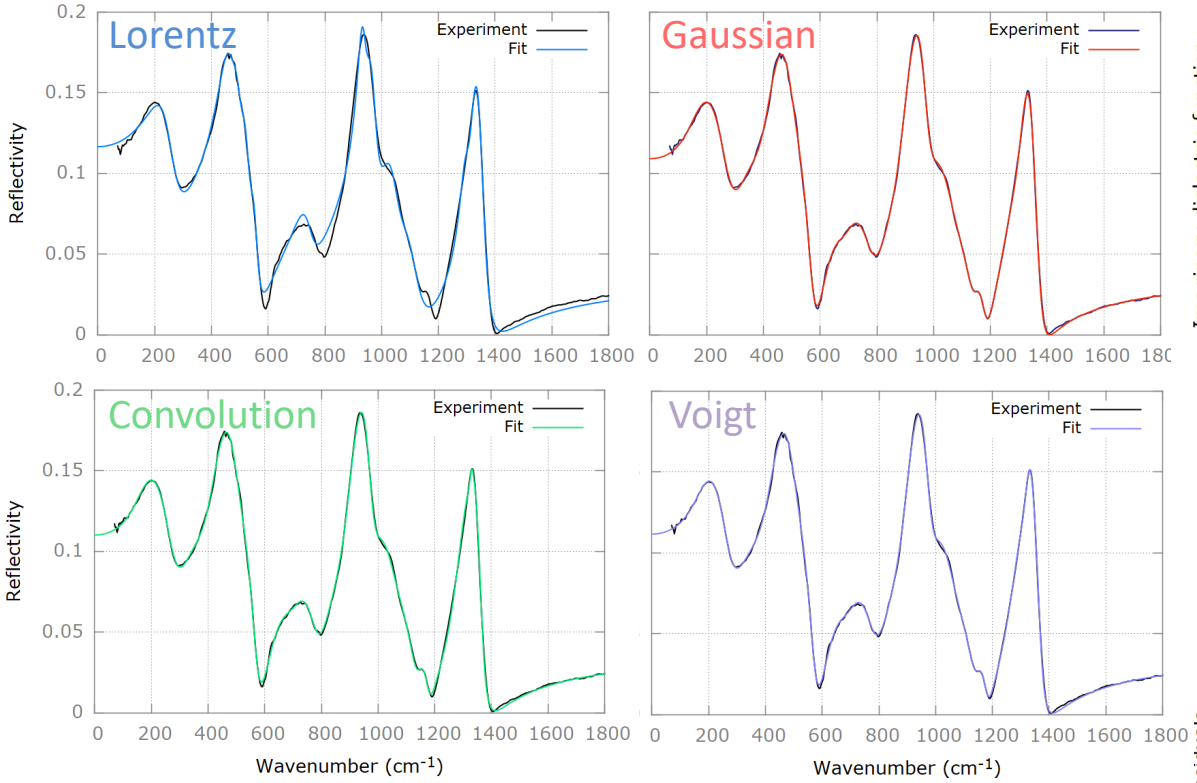

Imaginary dielectric function

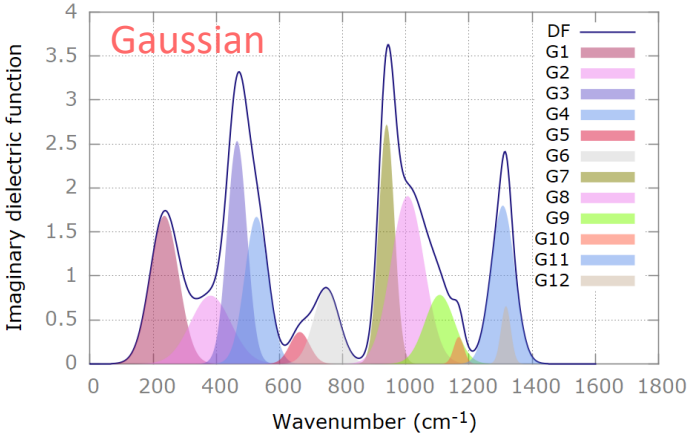

Fit residuals

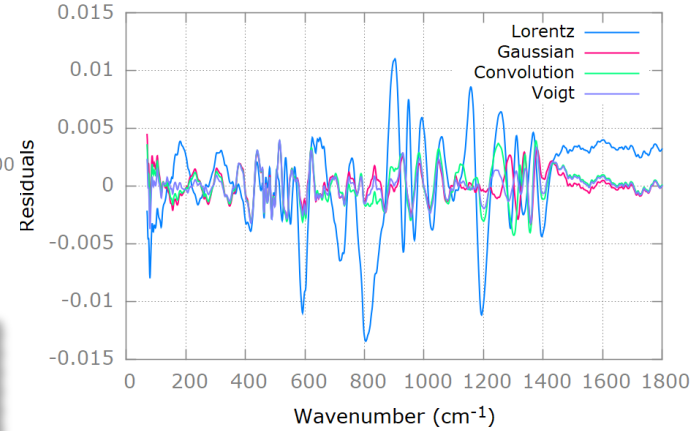

Convolution model

Voigt model

The causal Gaussian dielectric function model represents a good compromise in terms of quality of fit and simplicity for the analysis of the infrared response of most of glasses

Fits of reflectivity with a Gaussian dielectric function model

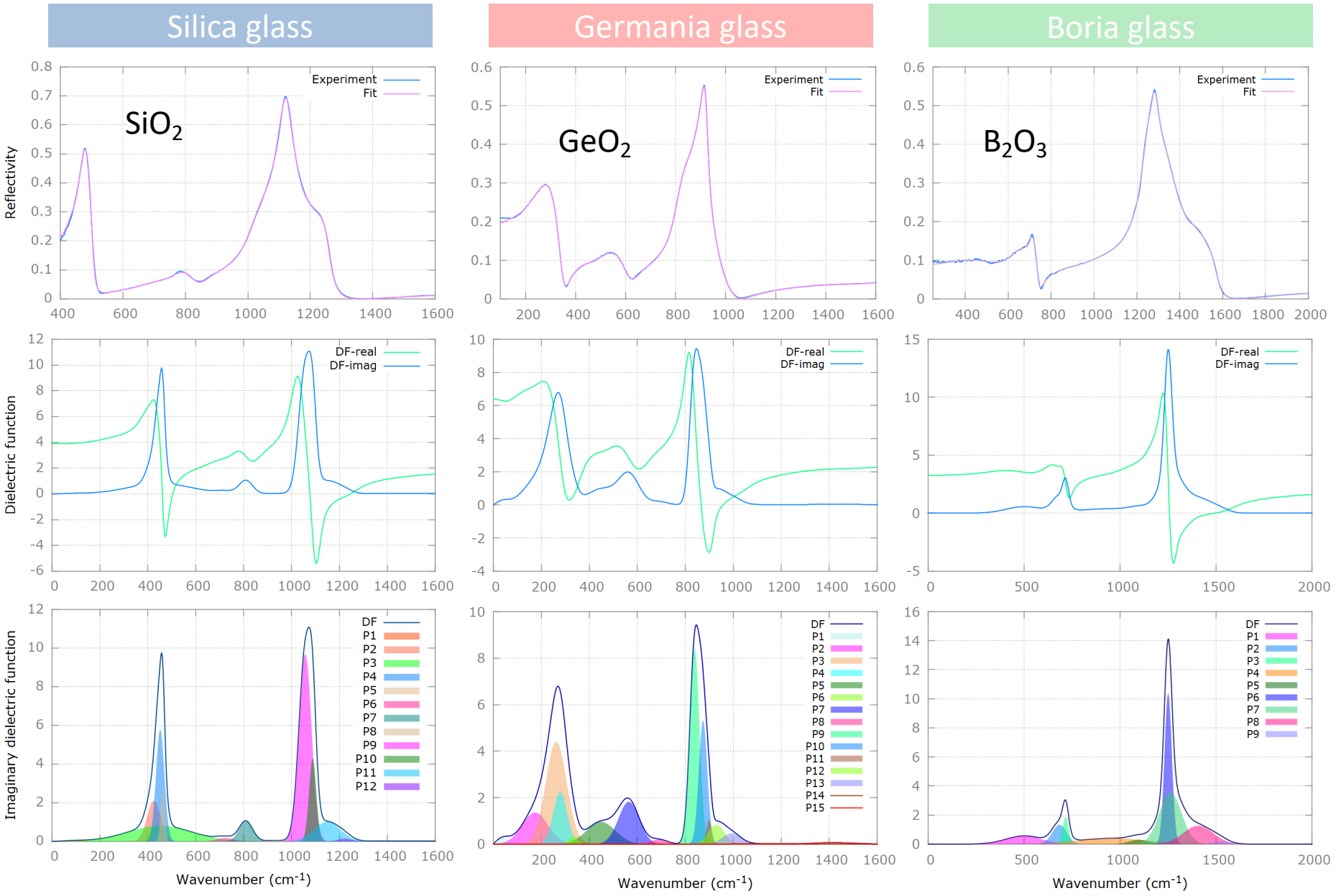

Fits of reflectivity with a Gaussian dielectric function model

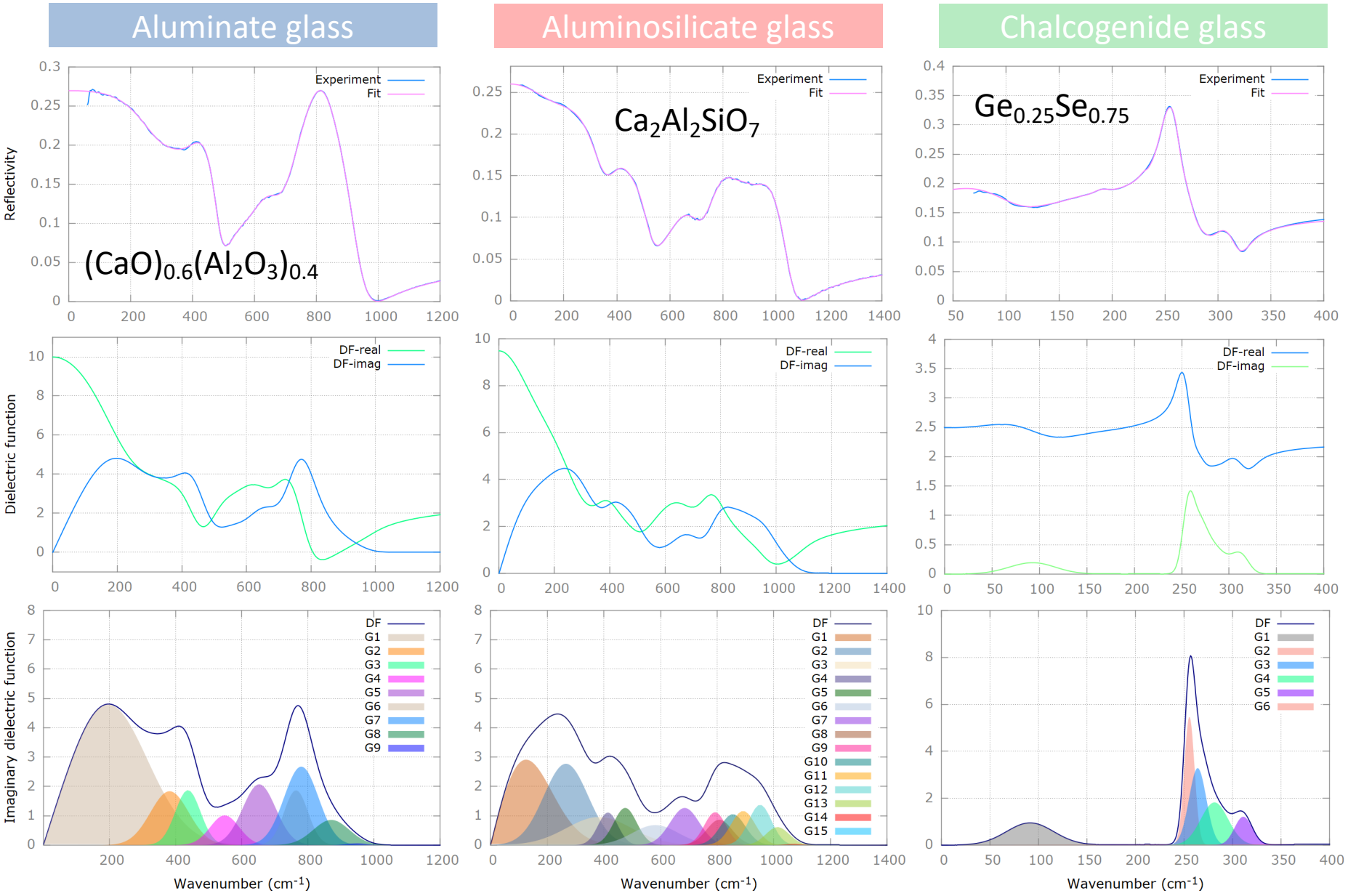

Fits of reflectivity with a Gaussian dielectric function model

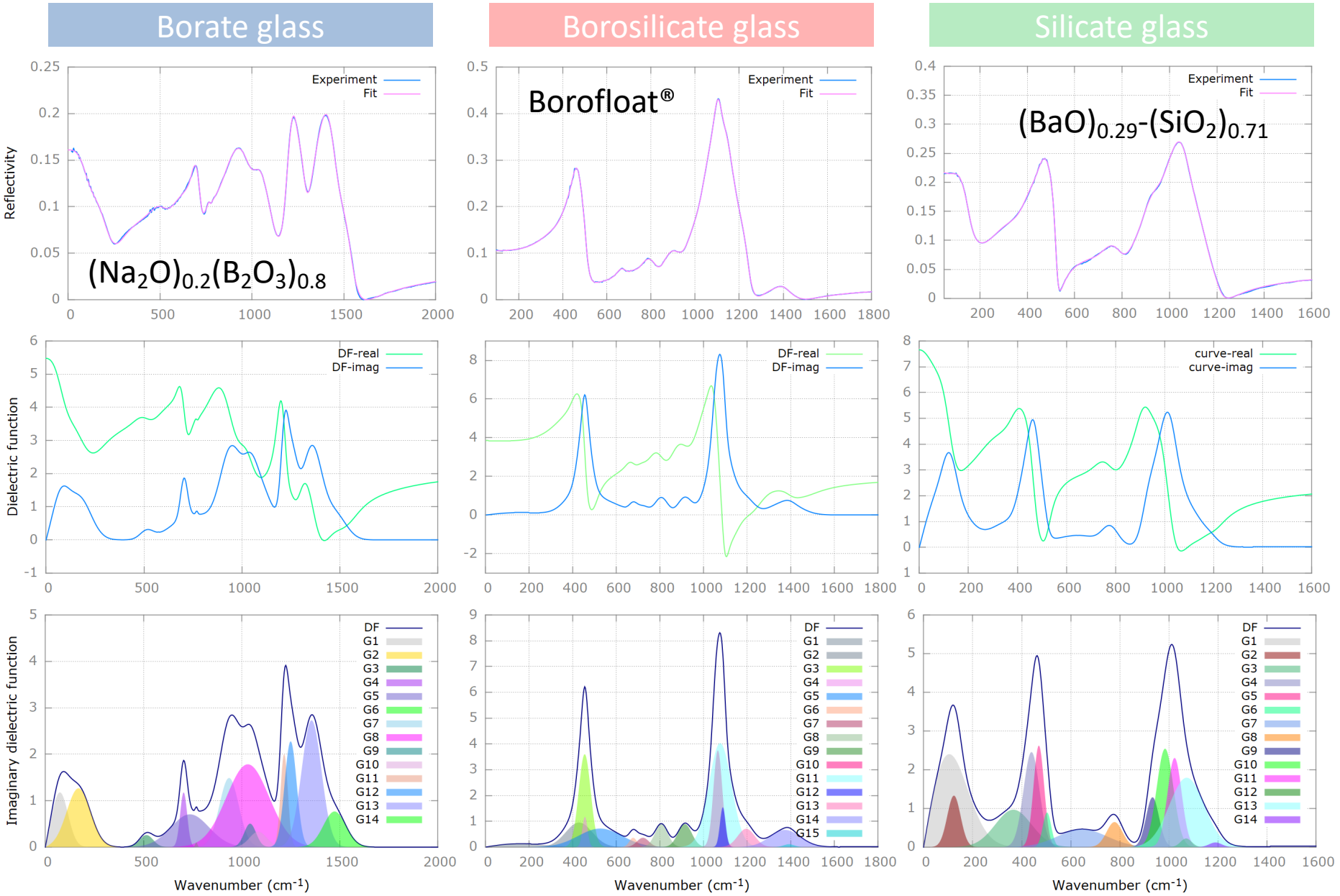

Infrared response of silicate glasses

Silicate glasses

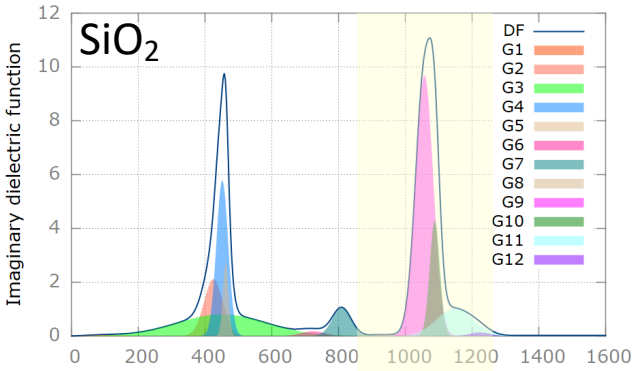

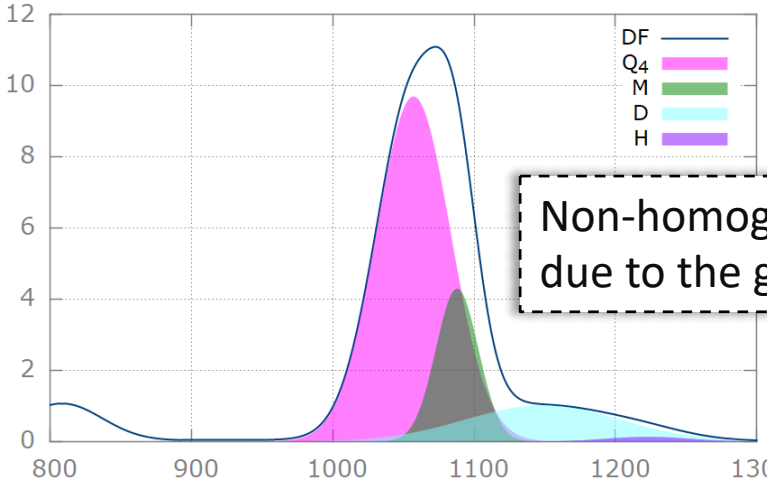

Non-homogeneous broadening due to the glass disorder.

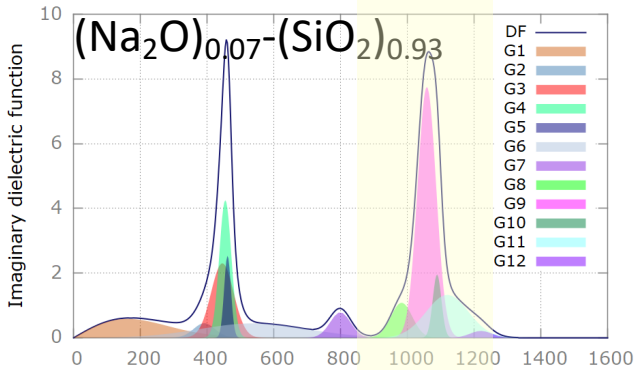

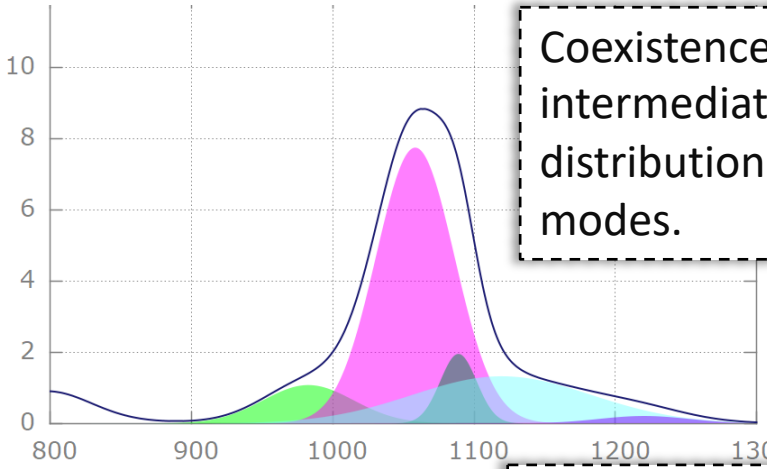

Coexistence of narrow, intermediate and wide distributions of vibrational modes.

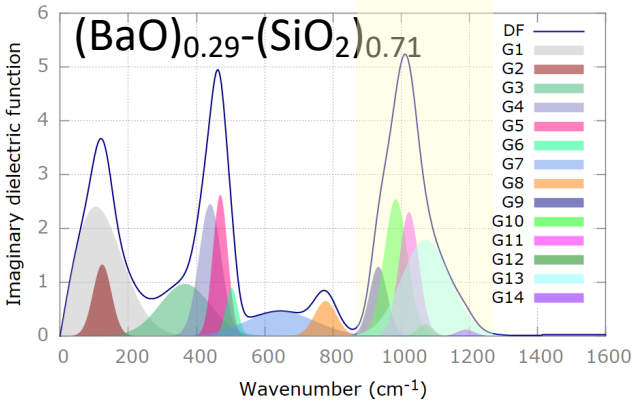

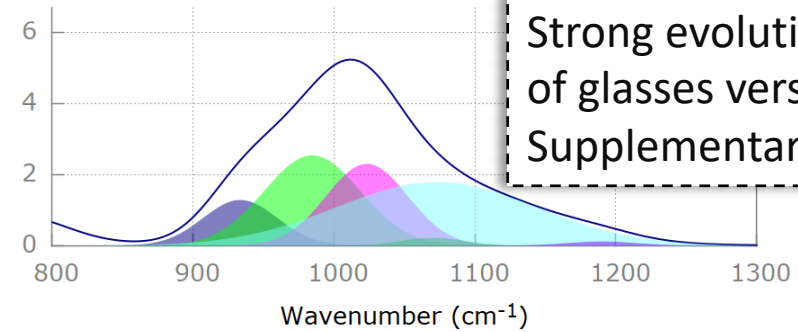

Strong evolution of the dynamics of glasses versus composition. Supplementary modes appear.

Infrared response of silicate glasses

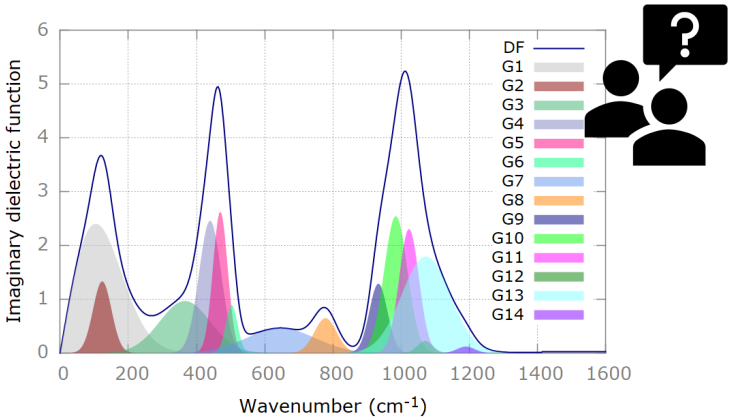

Why such a high number of Gaussian components?
Do they have a physical meaning?
What about the fidelity of the dielectric function model?
Does it include information on the glass network?
Can I probe cation modifiers?
…

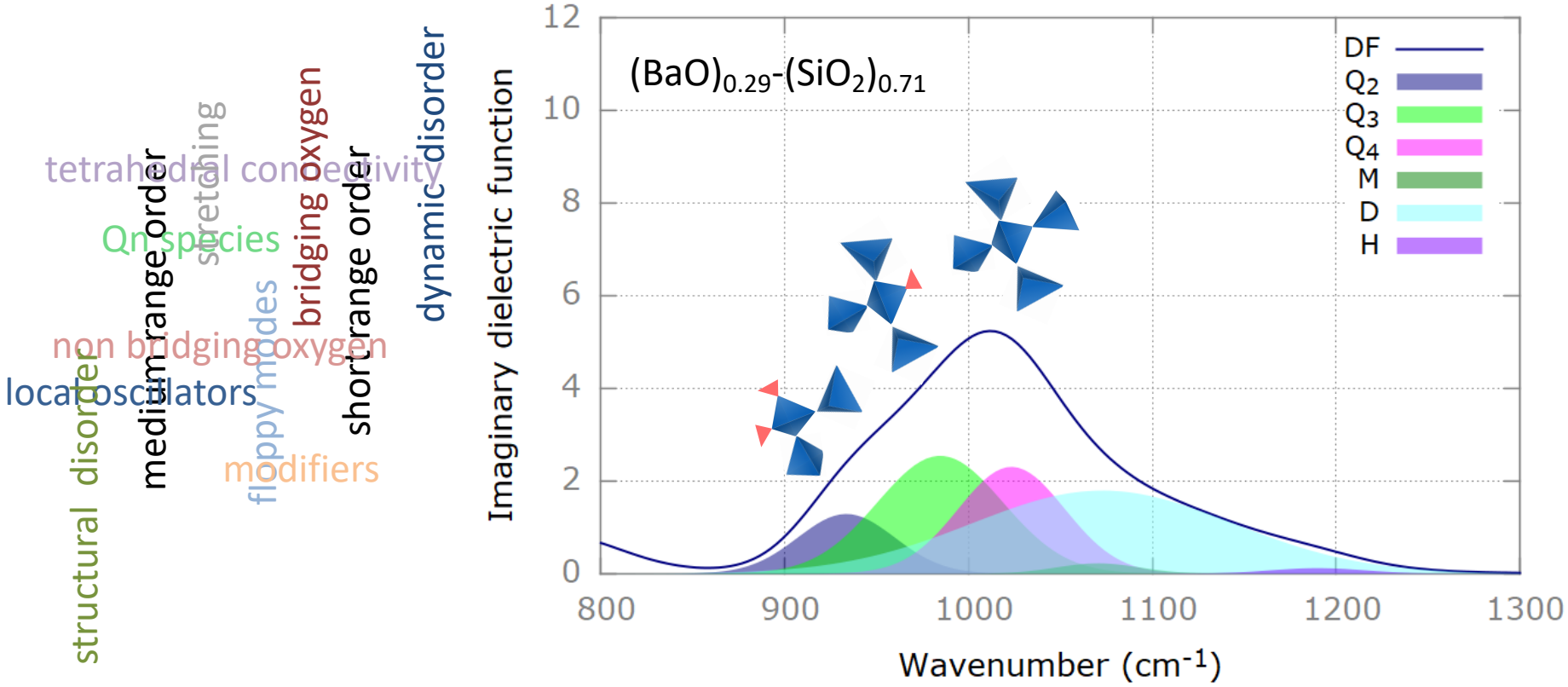

Inversion rate in $MgAl_2O_4$ versus temperature

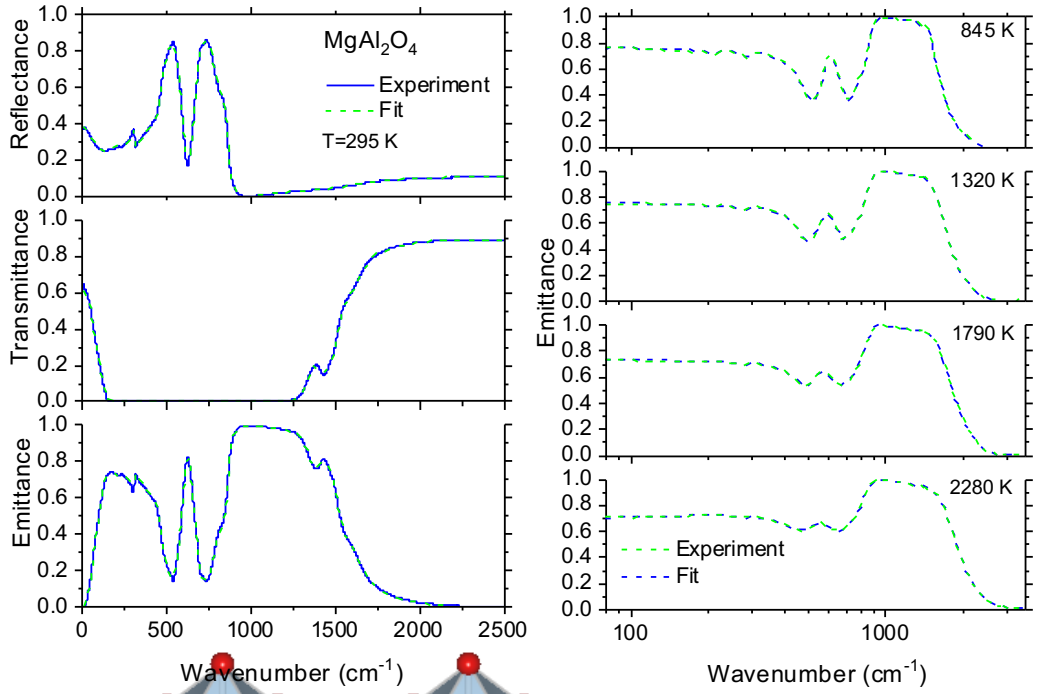

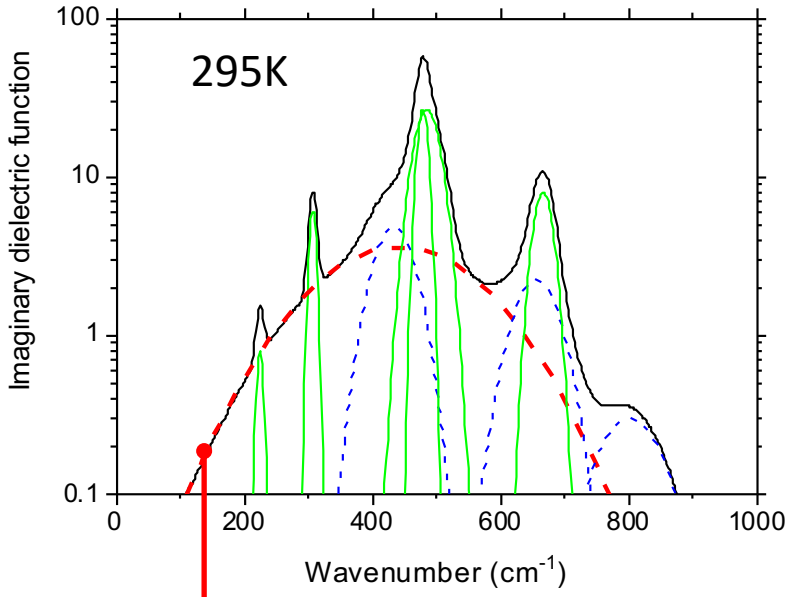

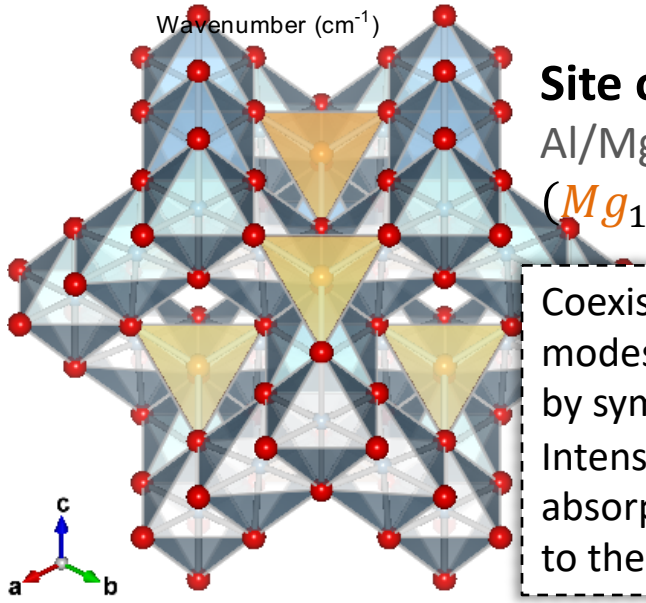

Site occupation disorder

Al/Mg disorder

$(Mg_{1-x}Al_x)[Mg_xAl_{2-x}]O_4$

Coexistence of allowed modes and modes forbidden by symmetry.

Intensity of the widest absorption component linked to the inversion rate x.

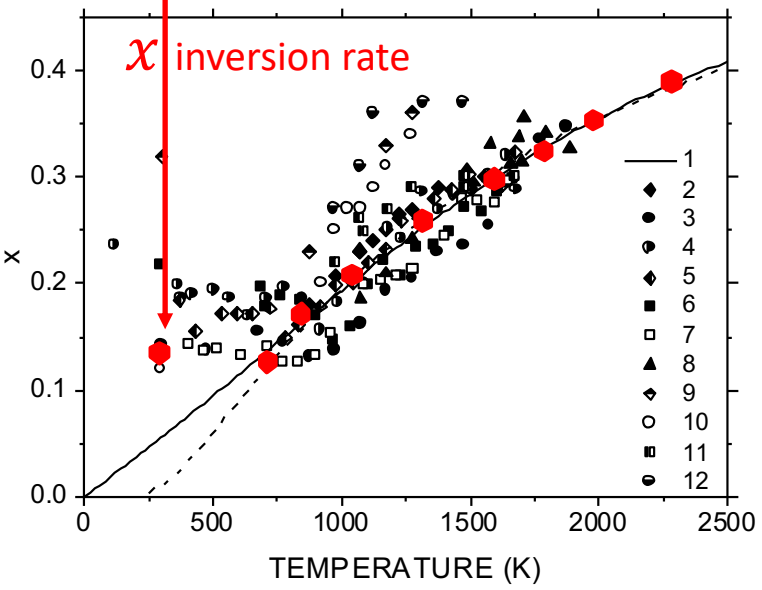

D. De Sousa Meneses et al. J. Phys. Cond. Mat. 18 5669-5686 2006

Dynamics and phase transitions of crystalline SiO_2

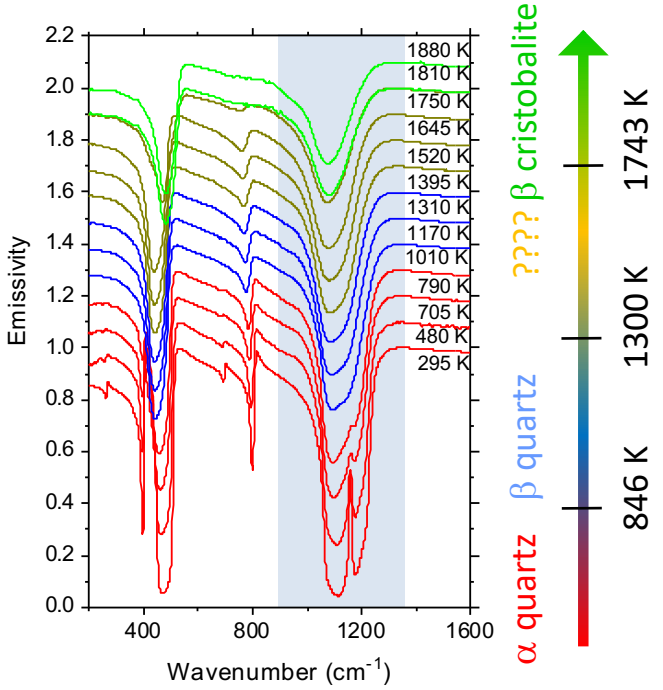

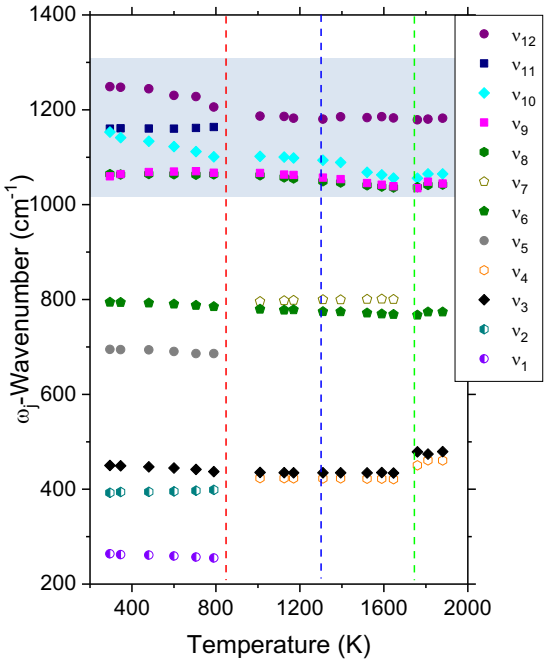

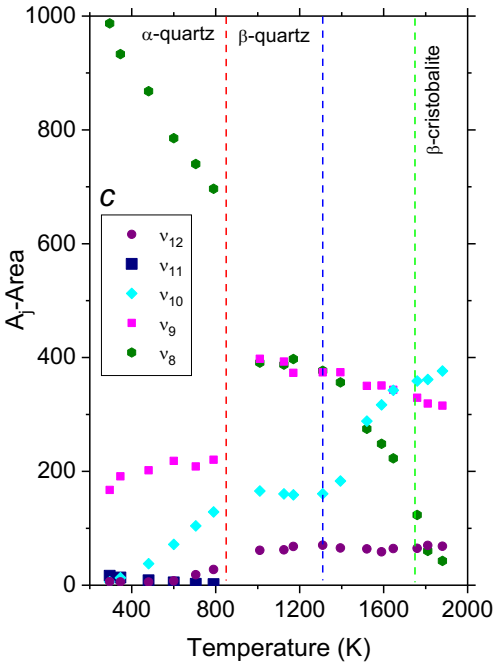

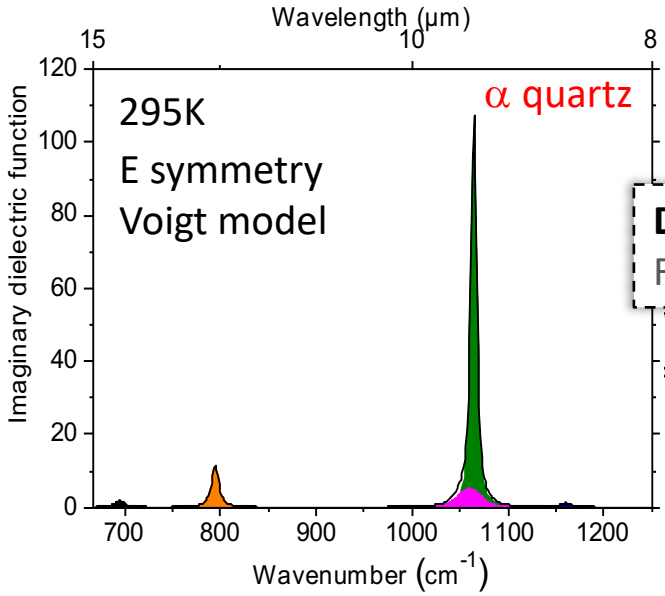

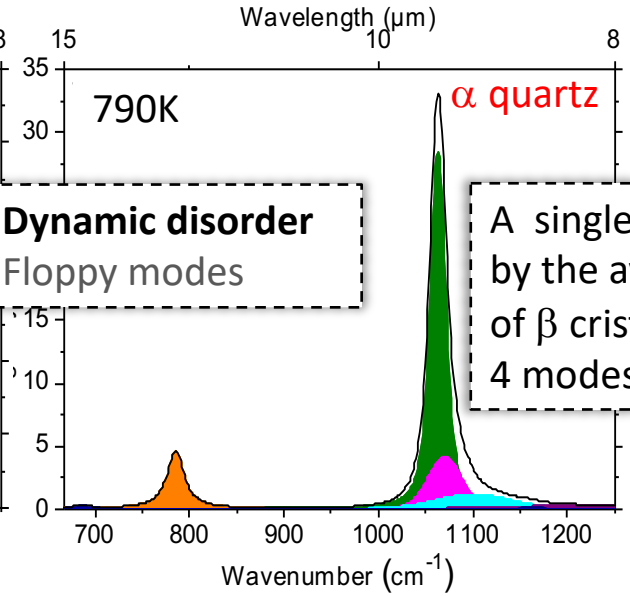

Dynamic disorder
Floppy modes

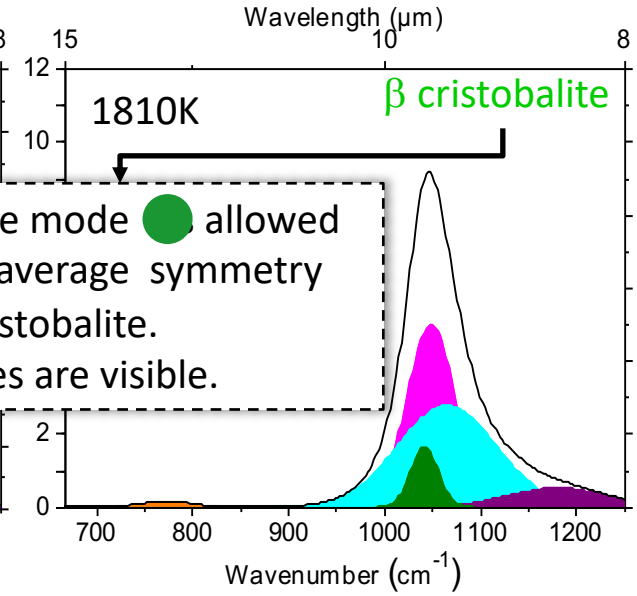

A single mode allowed by the average symmetry of β cristobalite.
4 modes are visible.

Dynamics of a silica glass versus temperature

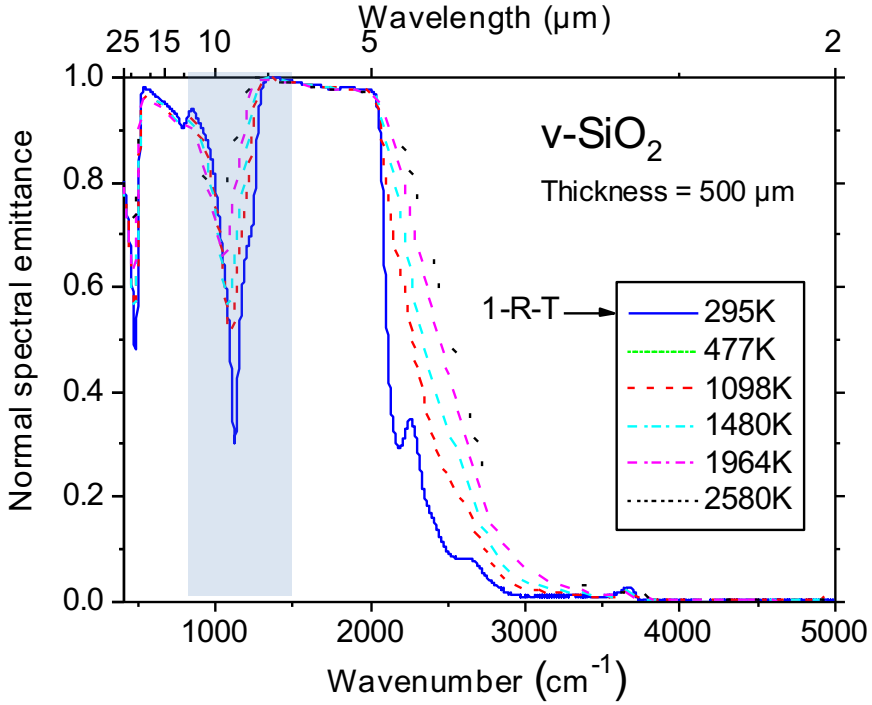

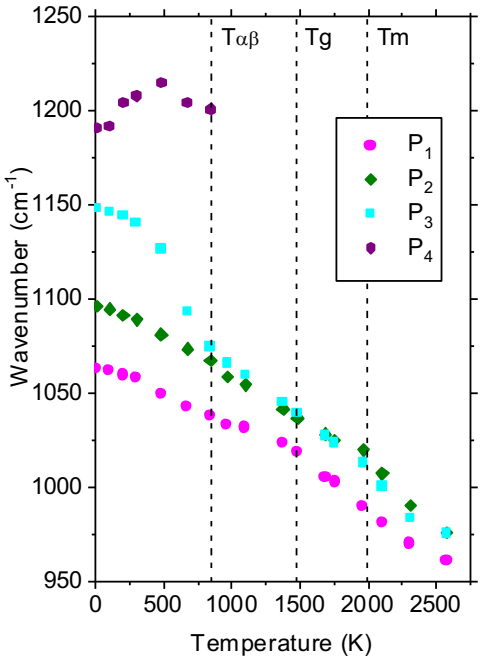

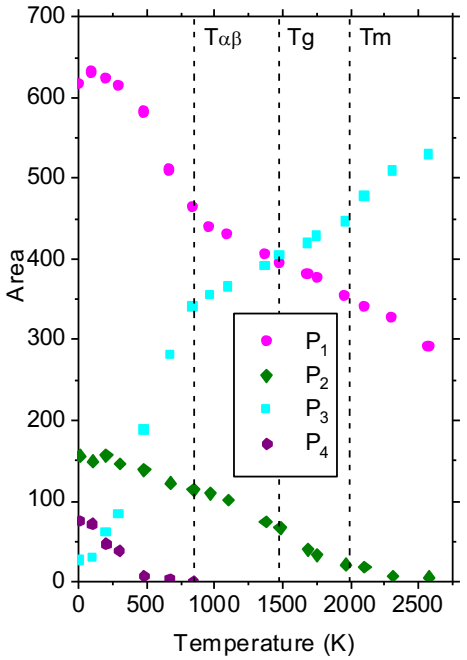

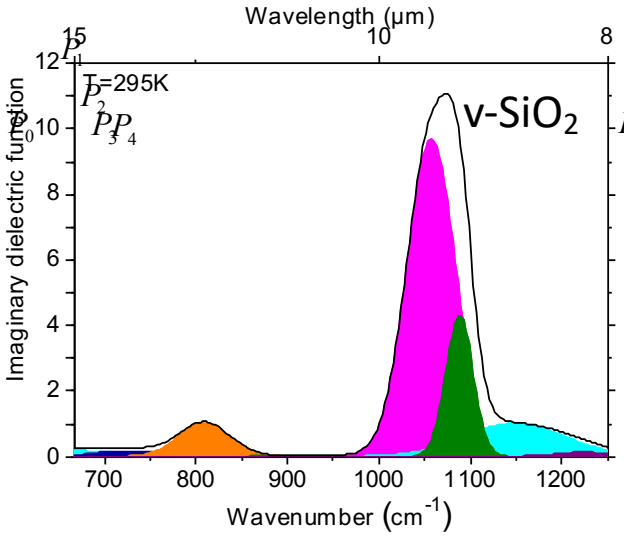

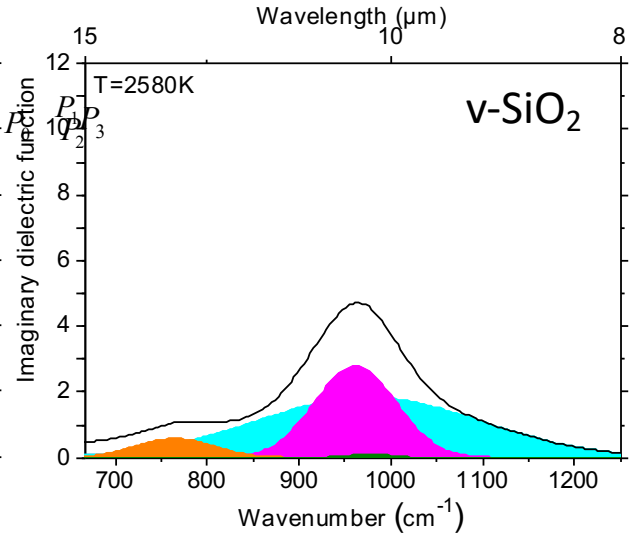

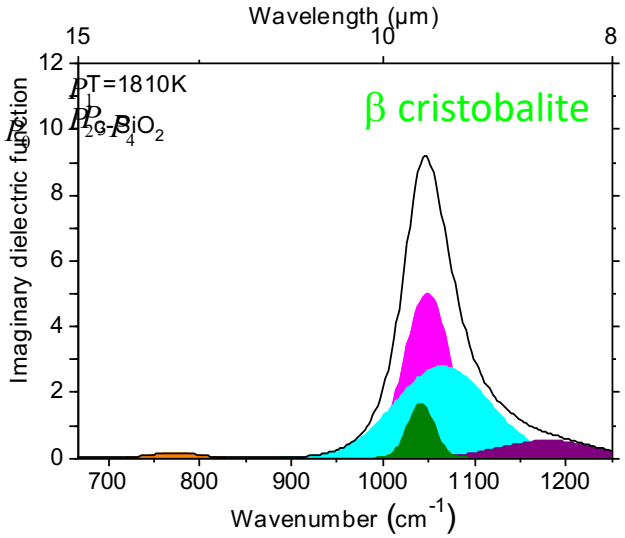

Infrared response of silicate glasses

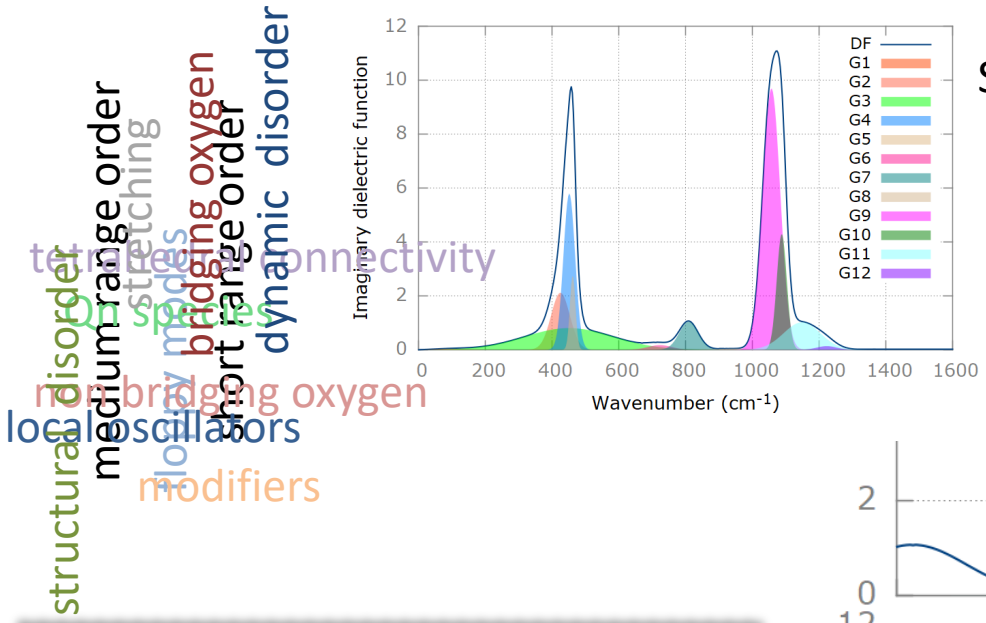

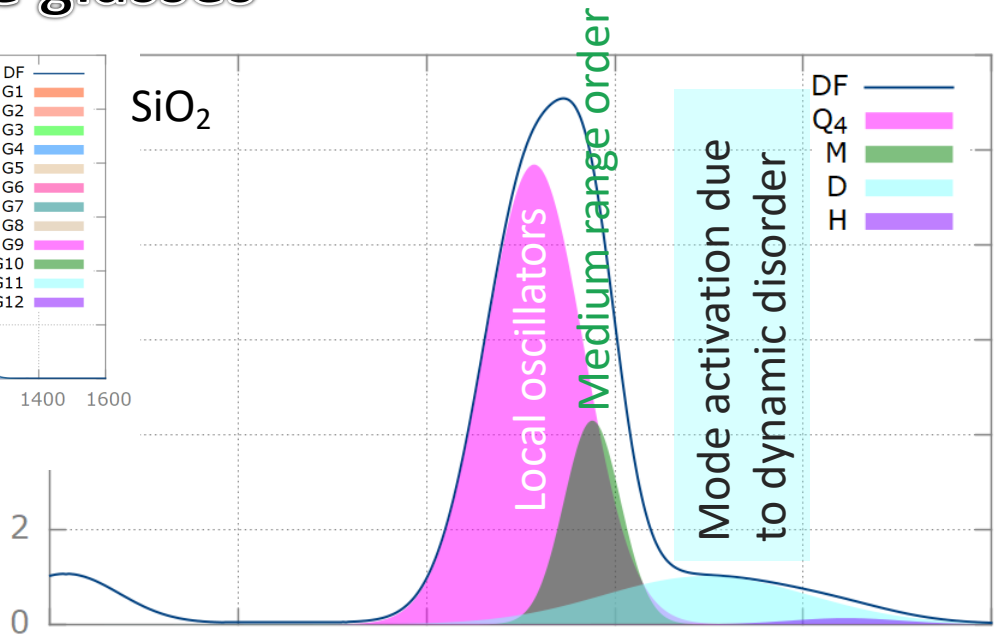

Gaussian components give information on the silicate network dynamics, cation motions, network connectivity, short and medium range order….

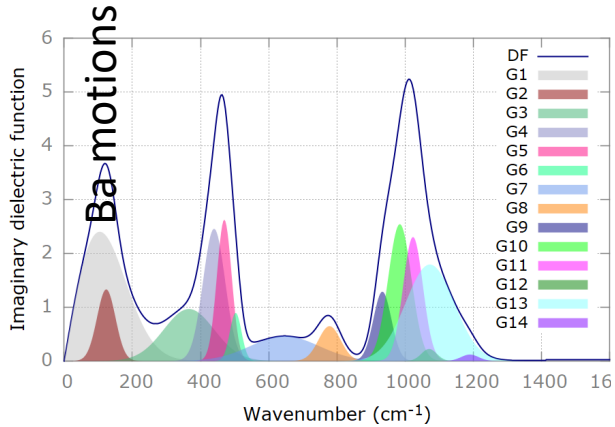

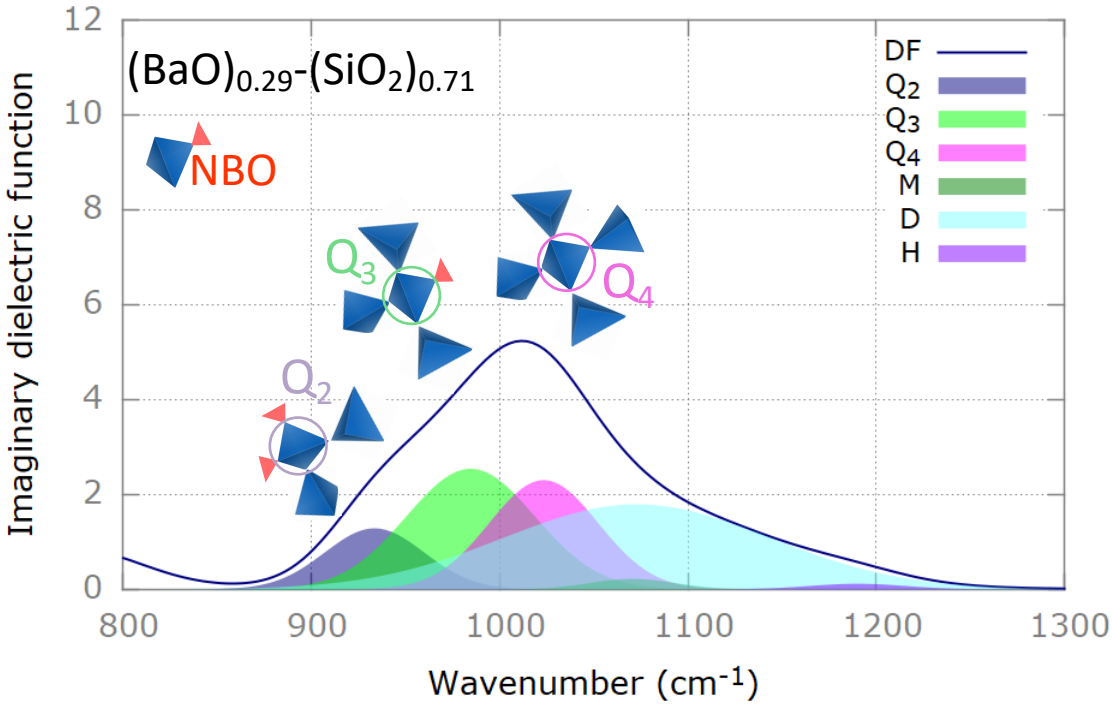

K_2O - SiO_2 glass system

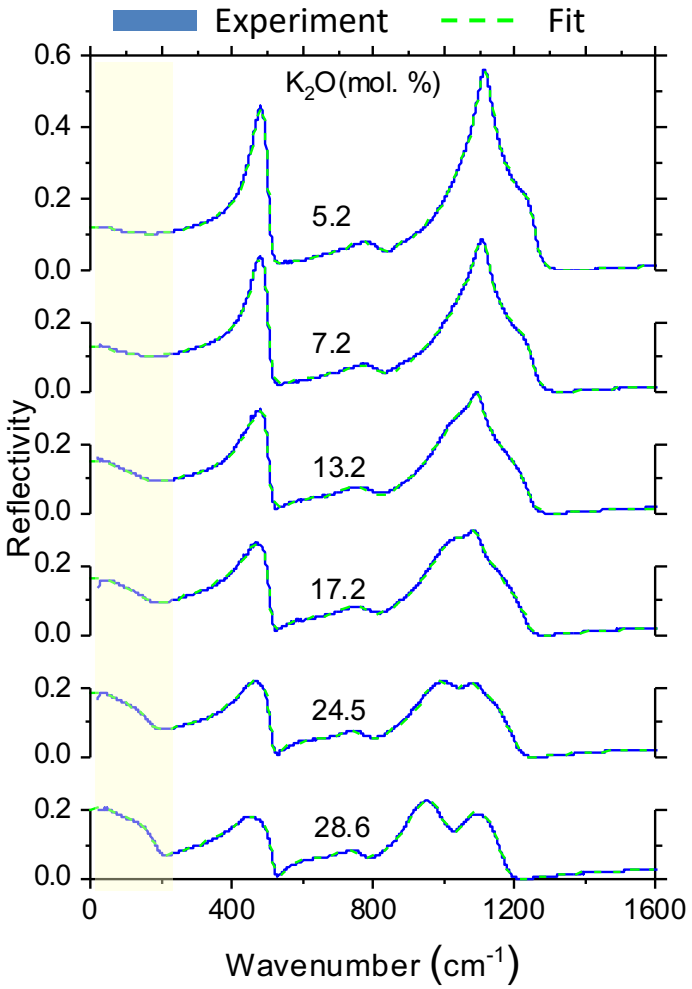

Strong evolution of the reflection spectrum with the increase of the K_2O content.

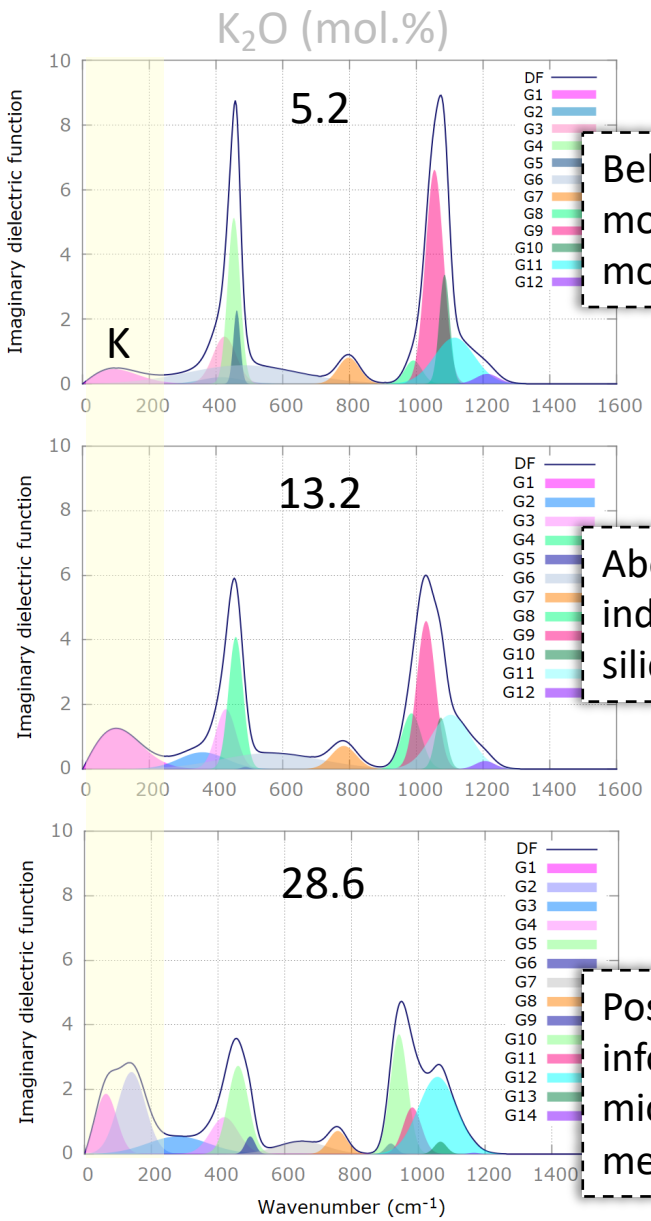

Below 200 cm^{-1}, vibrational modes are due to potassium motions.

Above 200 cm^{-1}, modes are induced by vibrations of the silicate network.

Possibility of extracting information on the glass microstructure at short and medium distances.

D. De Sousa Meneses et al Vibrational Spectroscopy 65 50-57 2013

K_2O - SiO_2 glass system

$$\varepsilon(\varpi) = \varepsilon_\infty + \sum_j \frac{2A_j}{\sqrt{\pi}}\left[D\left(2\sqrt{ln2}\,\frac{\varpi+\varpi_j}{\sigma_j}\right) - D\left(2\sqrt{ln2}\,\frac{\varpi-\varpi_j}{\sigma_j}\right)\right] + i\,A_j\left[exp\left(-4ln2\left(\frac{\varpi-\varpi_j}{\sigma_j}\right)^2\right) - exp\left(-4ln2\left(\frac{\varpi+\varpi_j}{\sigma_j}\right)^2\right)\right]$$

Dawson function: $D(x) = \exp(-x^2)\int_0^x \exp(t^2)dt$

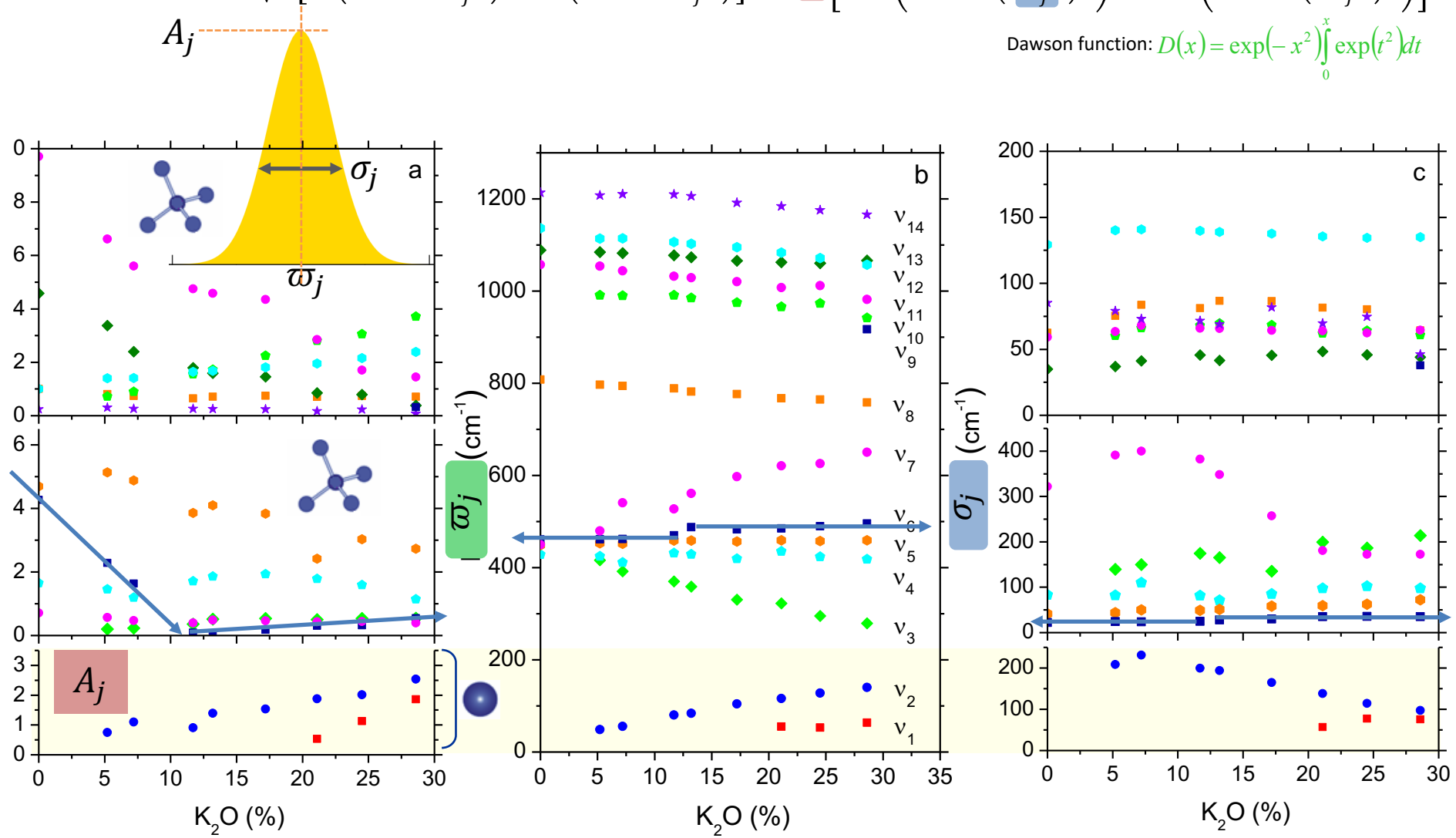

K_2O - SiO_2 glass system : short range order

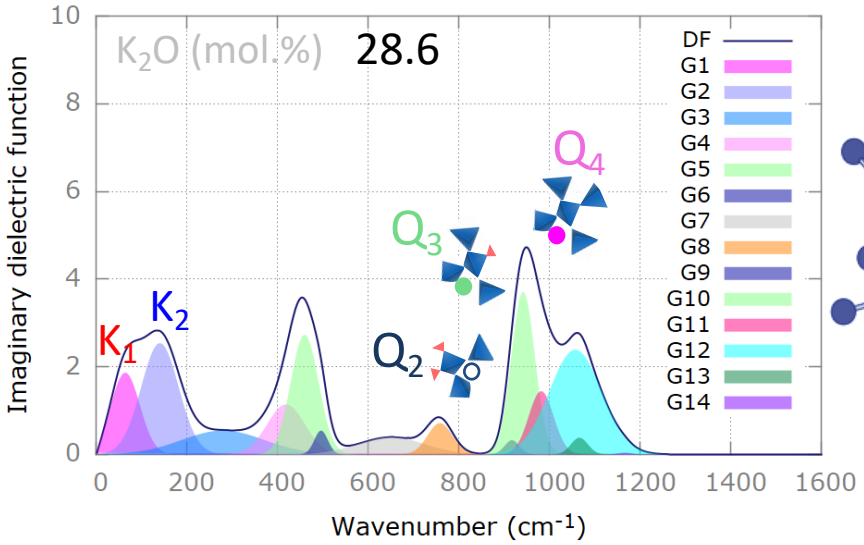

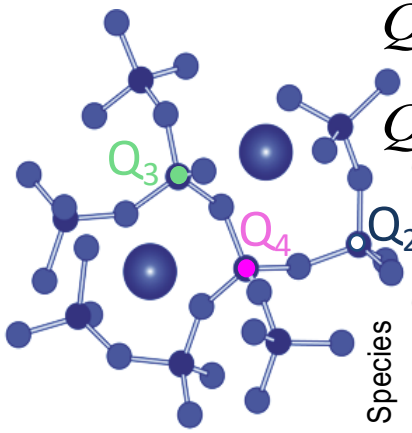

Q_n : tetrahedra with n bridging oxygens

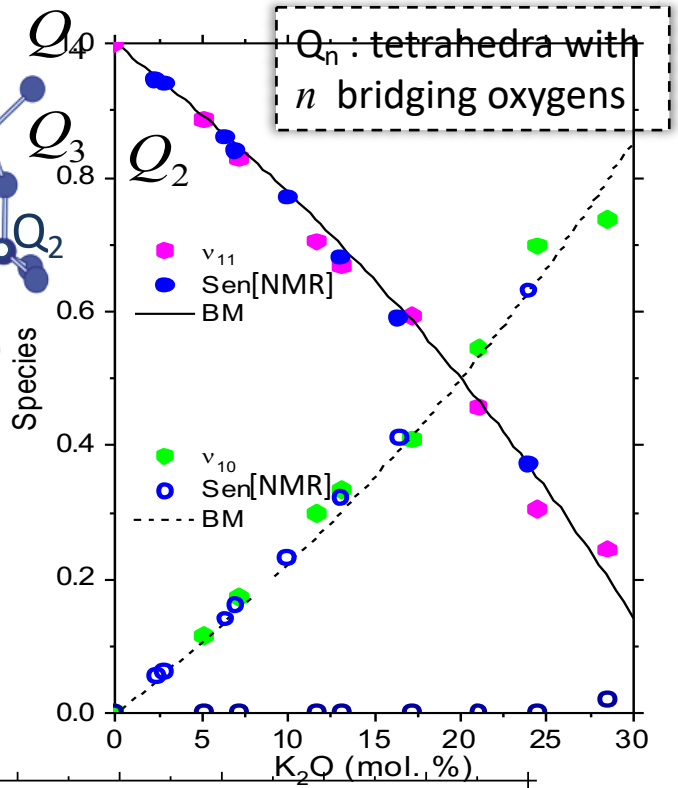

Sites of potassium cations

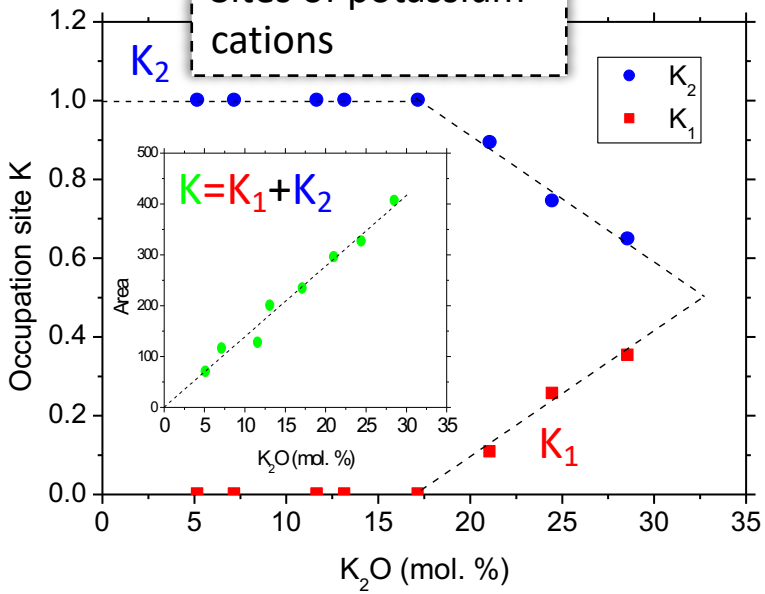

Bridging and non-bridging oxygen

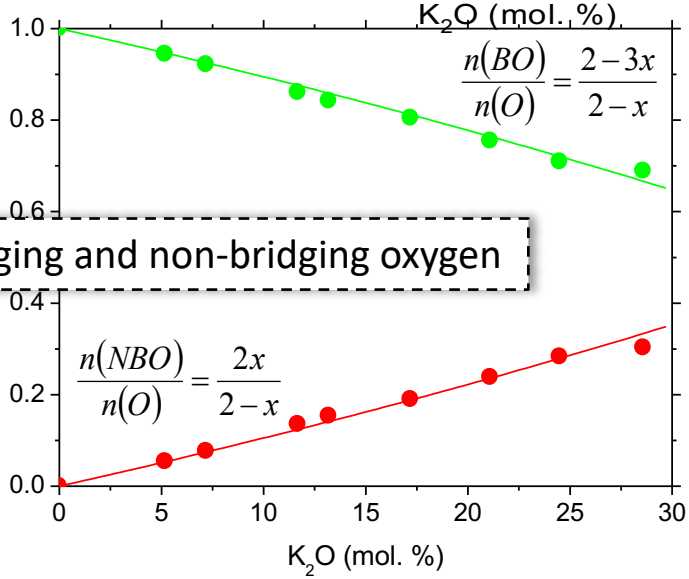

[NMR] Sen S, Youngman R E 2003 *J. Non-Cryst. Solids* 331 100

[BM] Binary model

K_2O - SiO_2 glass system : medium range order

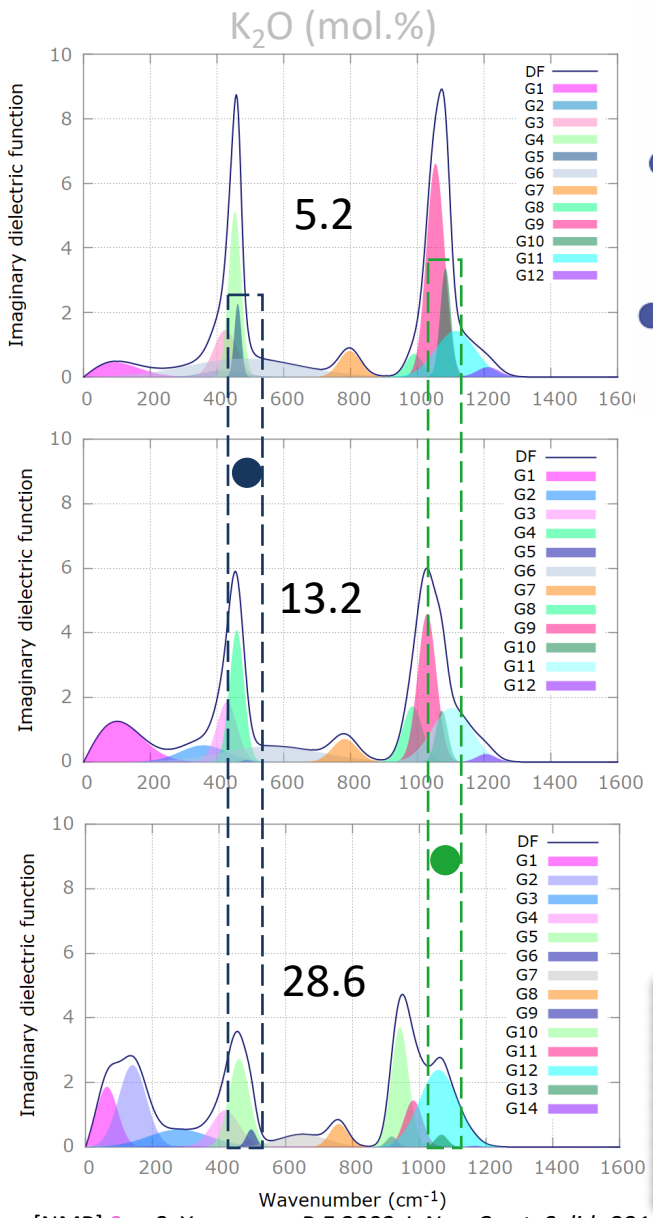

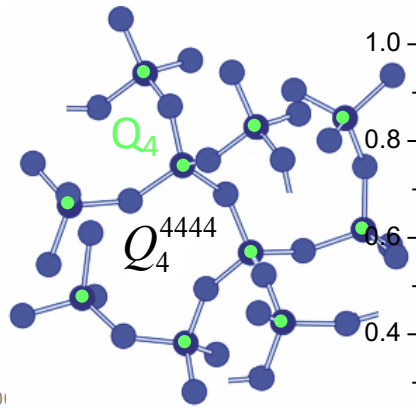

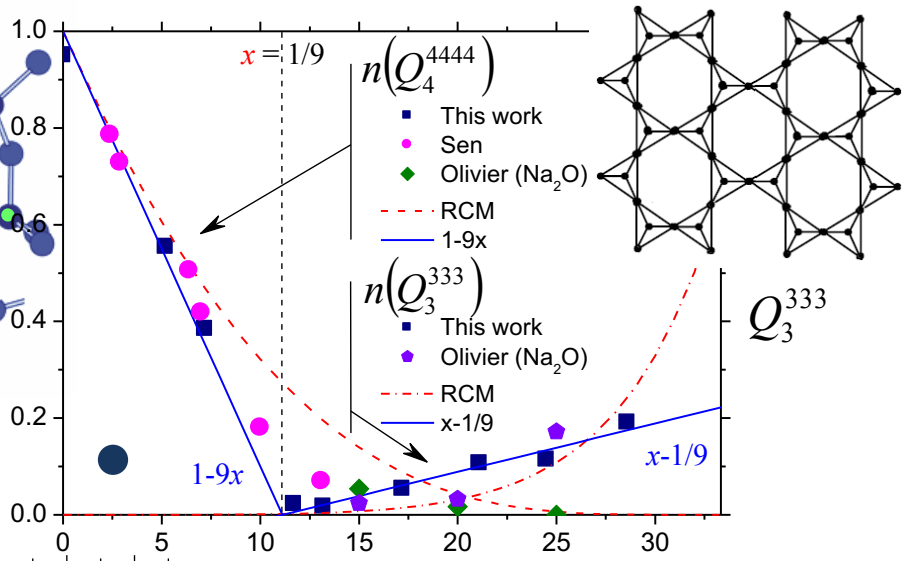

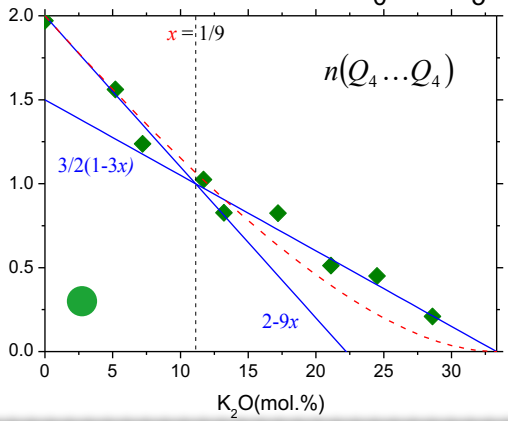

Random Connectivity Model does not explain the glass structure. Depolymerization follows a specific path.

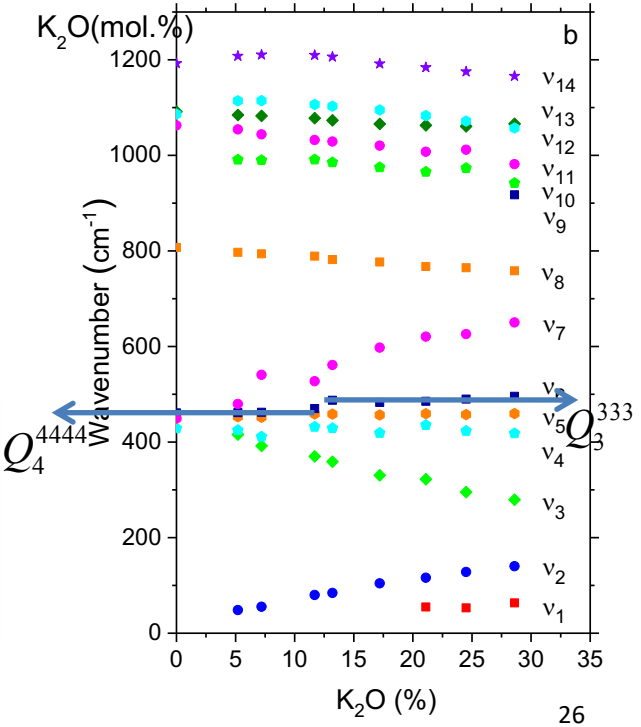

[NMR] Sen S, Youngman R E 2003 *J. Non-Cryst. Solids* 331 100

[NMR] Olivier L, Yuan X, Cormack A N, Jäger C 2001 *J. Non-Cryst. Solids* 293-295 53

SiO_2 thin film implanted with Krypton

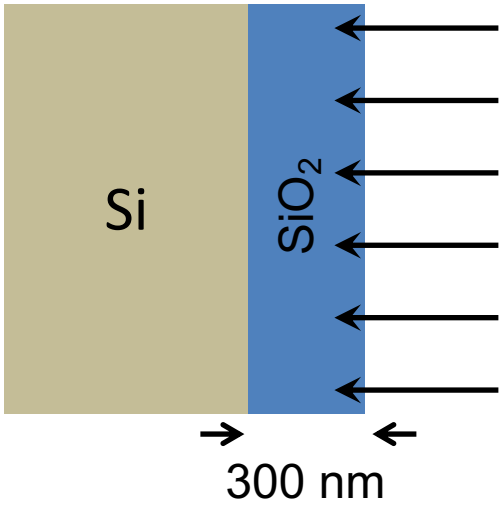

Krypton implantation

220 KeV

510^{16} Kr/cm^2

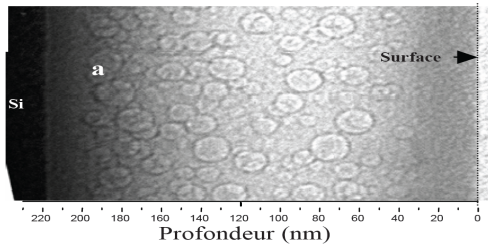

Static relative permittivity versus annealing temperature

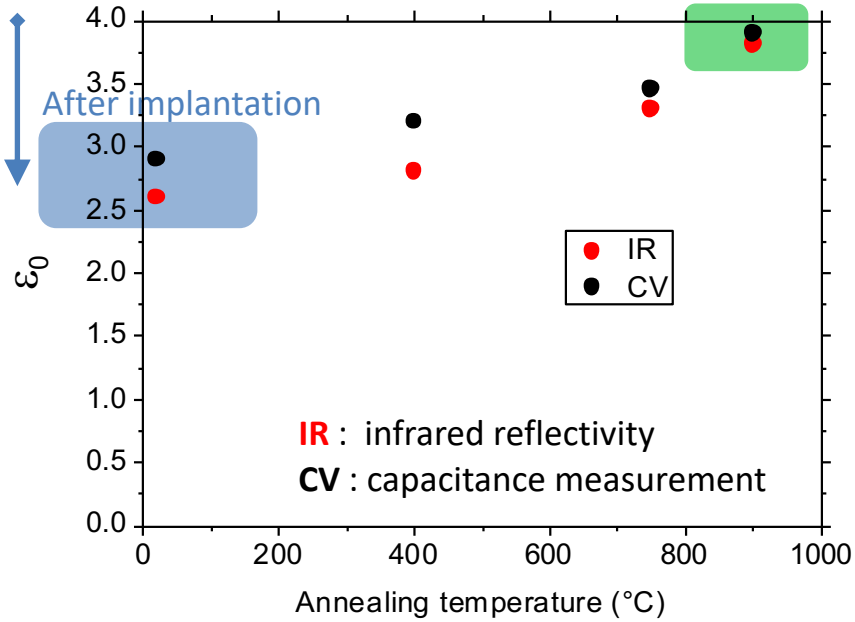

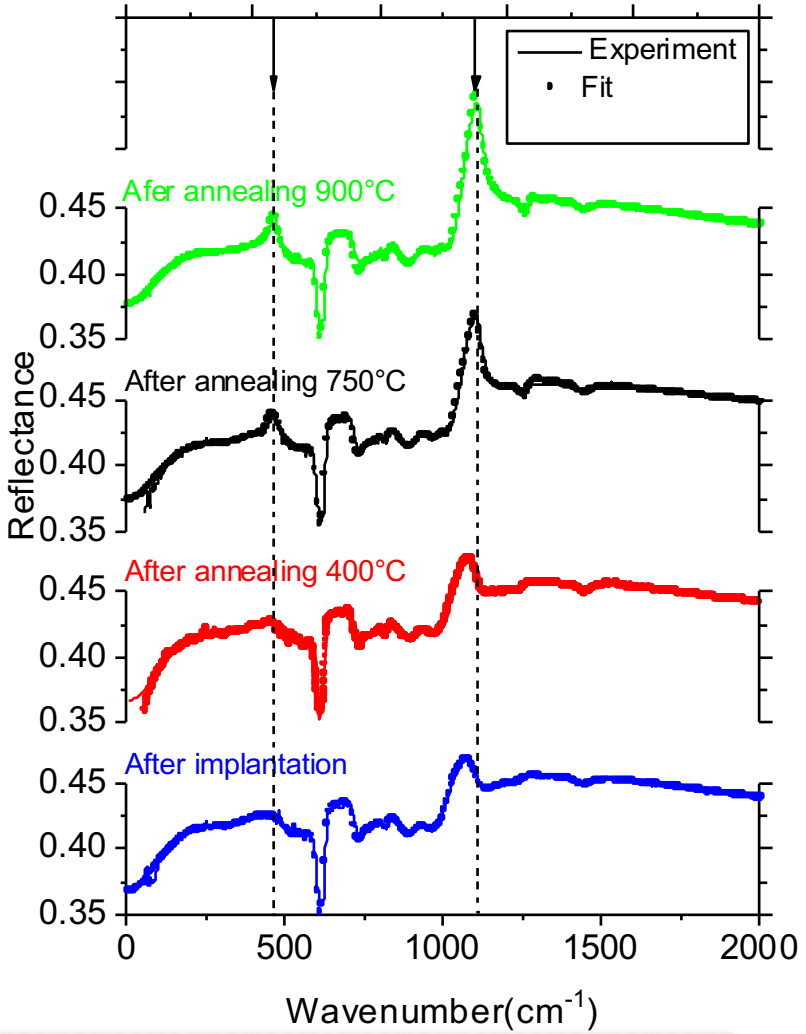

Strong decrease of the static relative permittivity of the SiO_2 thin film after implantation.

Material healing after annealing at 900 ° C

SiO_2 thin film implanted with Krypton

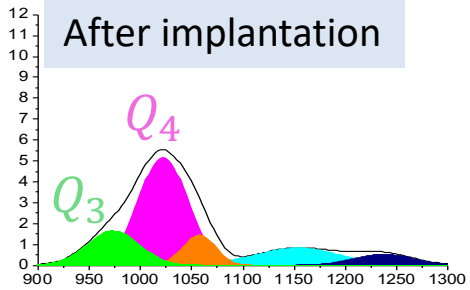

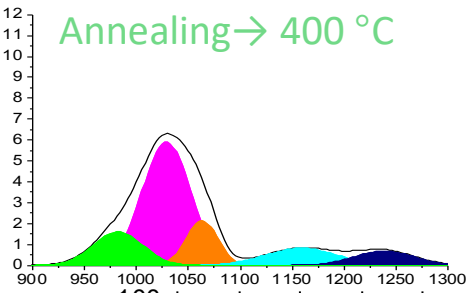

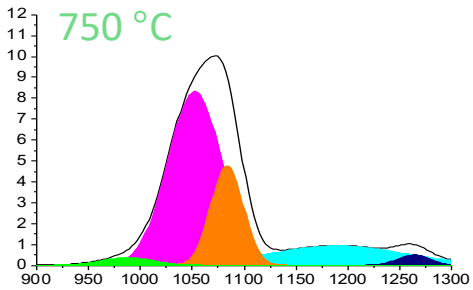

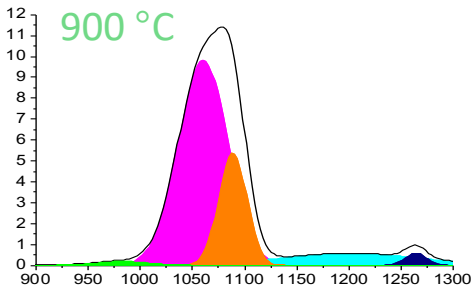

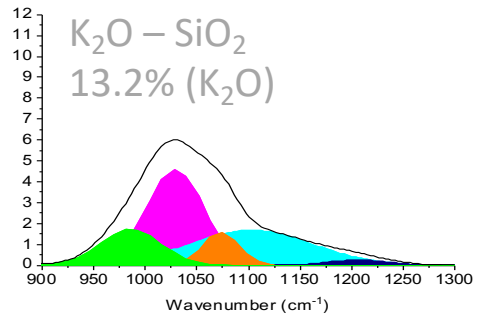

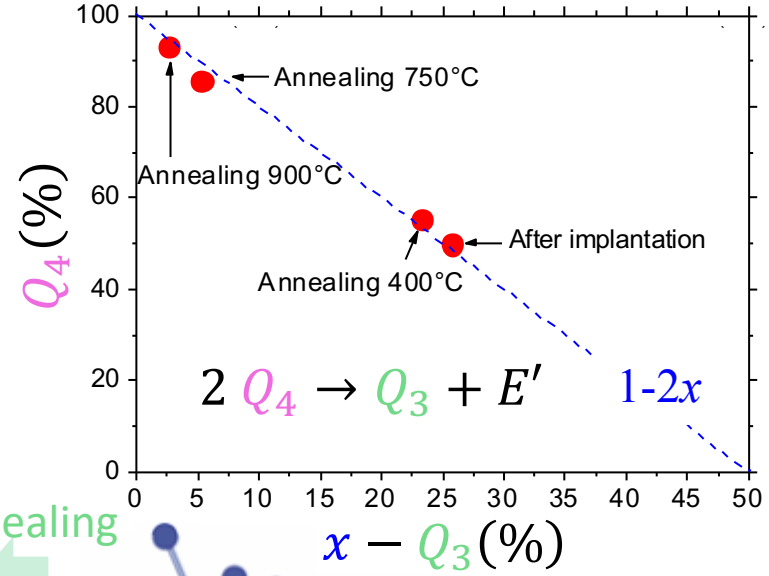

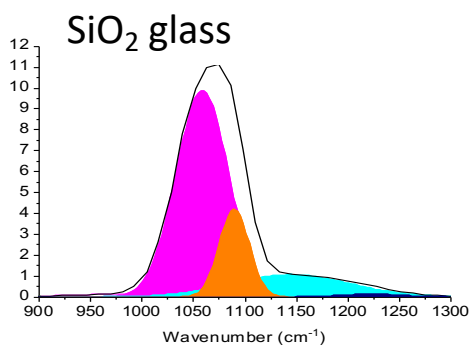

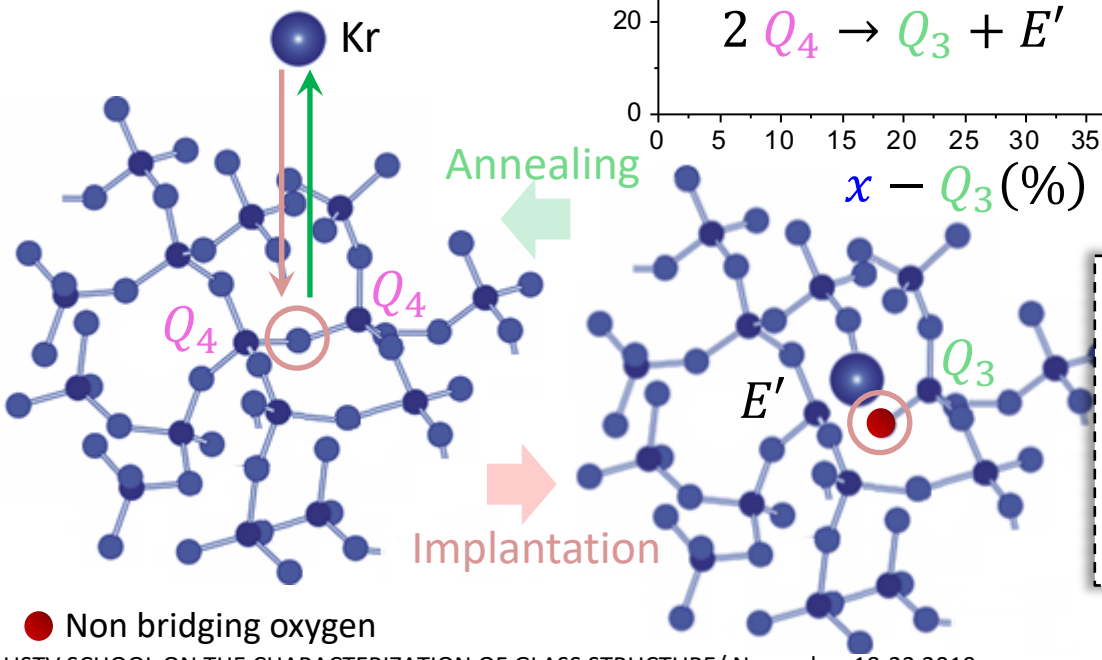

Implantation mechanism

Damage of the silicate network by creating E' centers and Q_3 structural units.

Loss of 50% of the Q_4 structural units inducing a diminution of the vibrational contribution to the static permittivity.

Structural relaxation of a silicate glass

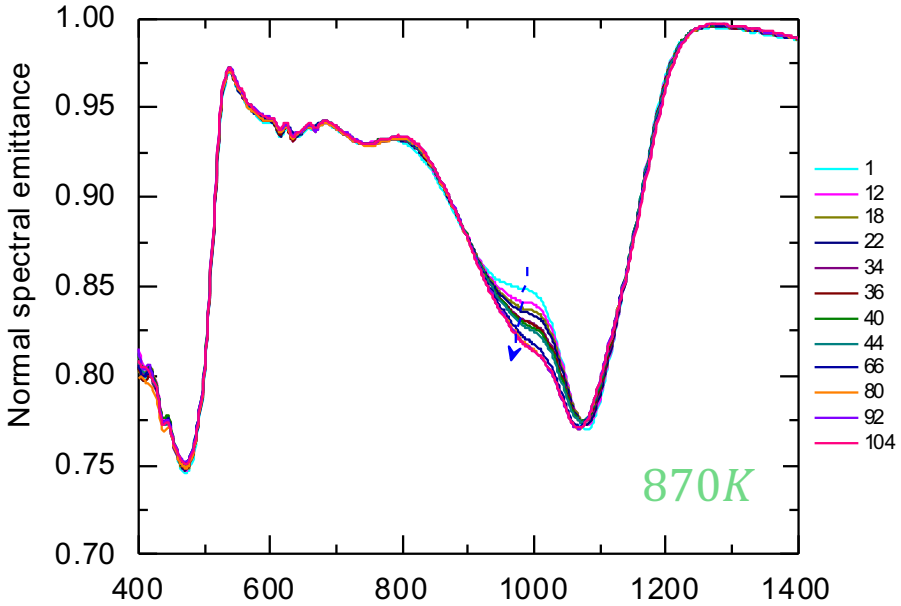

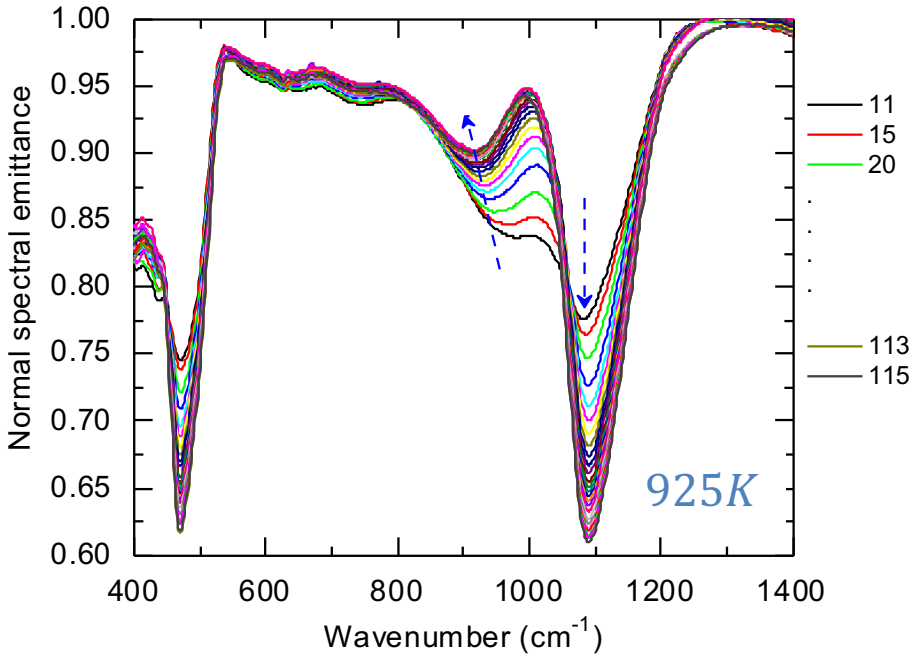

$(Na_2O)_{0.27}\ (SiO_2)_{0.73}$ silicate glass

Thermal heat treatment

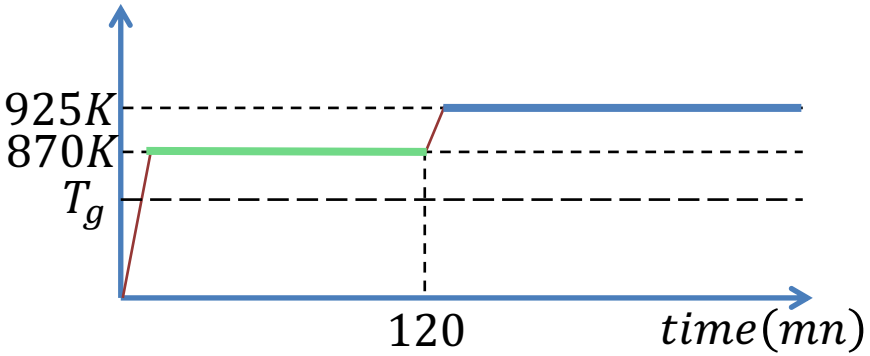

Glass transition temperature (T_g): $\cong 730K$
Continuous acquisition of spectra during annealing at 870 K and 925K

Structural relaxation of a silicate glass

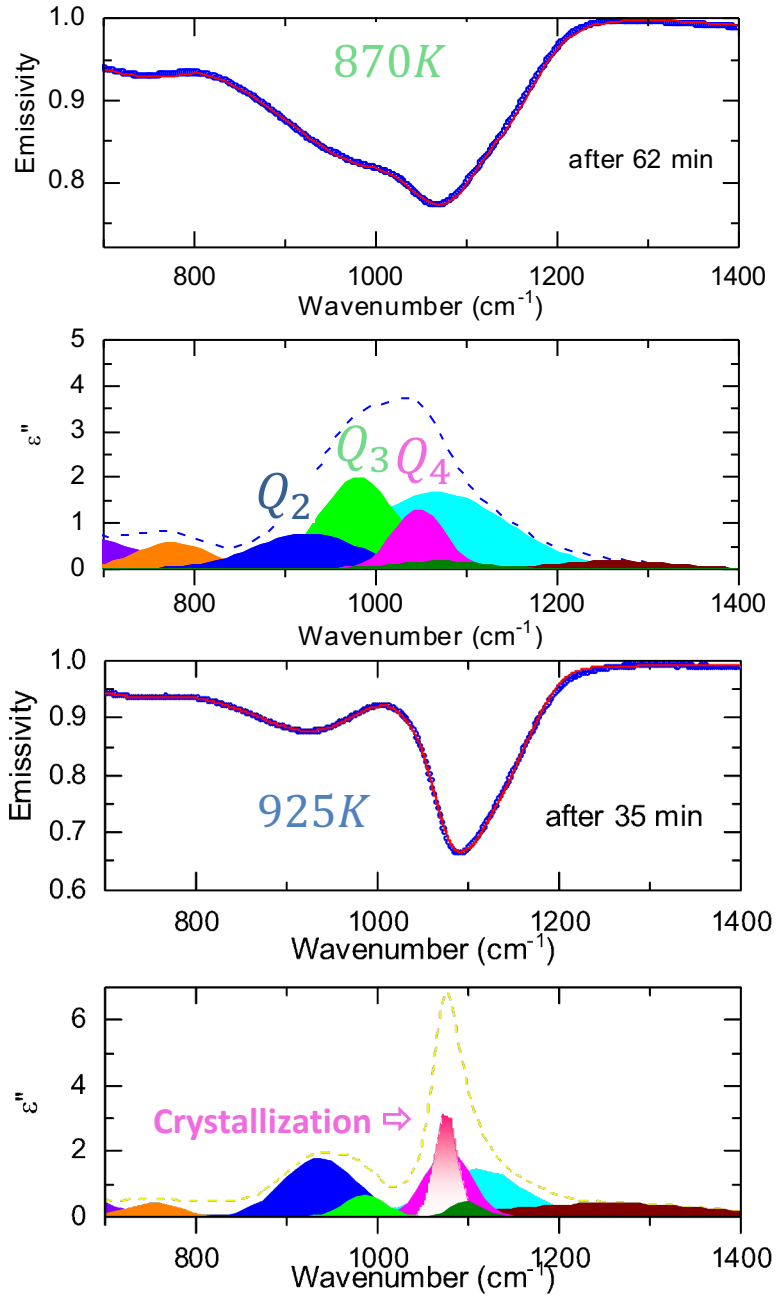

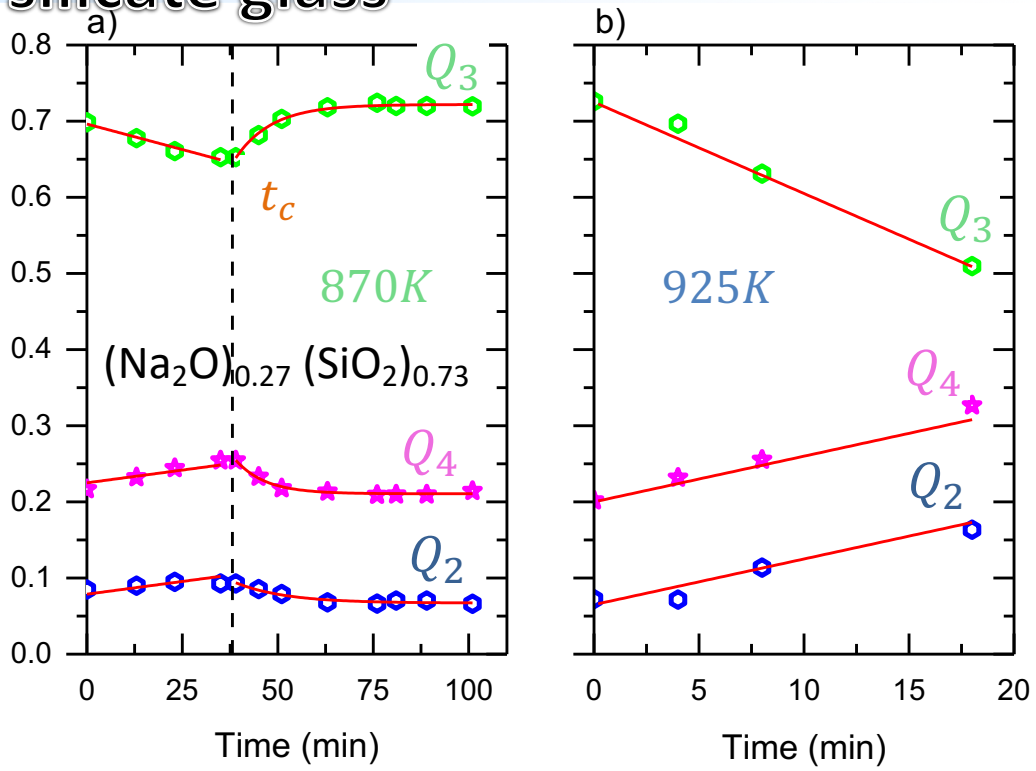

Annealing at 870 K does not lead to crystallization of the glass. $2Q_3 \Leftrightarrow Q_2 + Q_4$

First step, small shift of the chemical equilibrium to the right.

After t_c, structural relaxation ($\tau \cong 10\ mn$) and shift to the left of the chemical equilibrium.

$$Q_n(t) = c_n \exp\left(-\frac{t - t_c}{\tau}\right) + d_n$$

At 925 K crystallization is evidenced after 20 mn.

Infrared response of aluminosilicate glasses

$Ca_2Al_2SiO_7$ glass

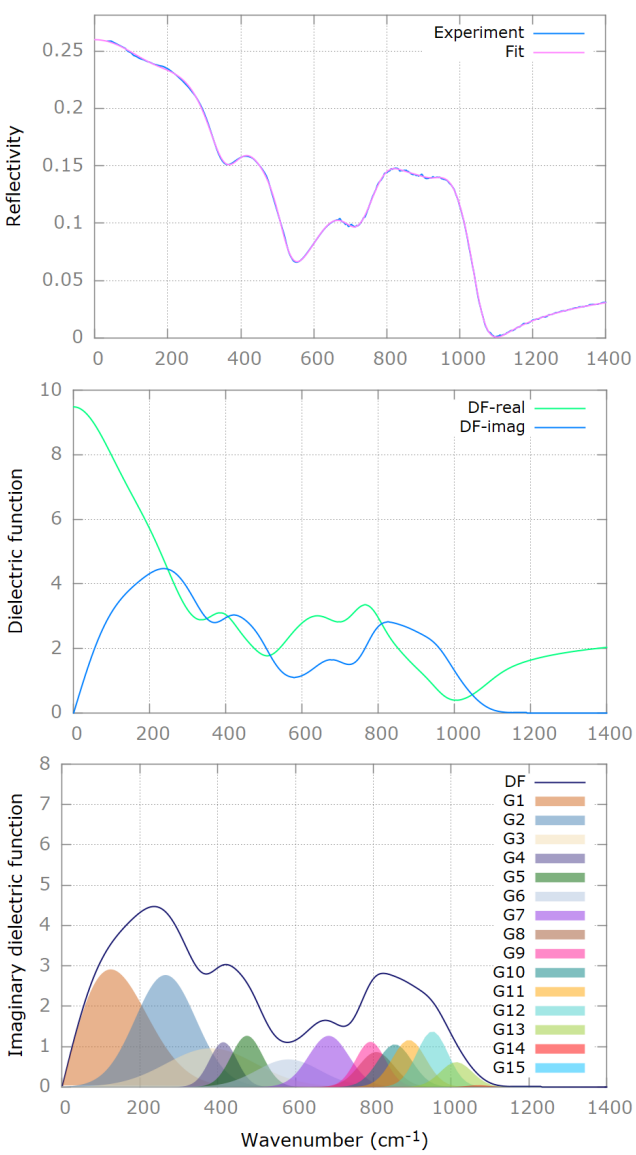

$BaAl_2Si_2O_8$ glass

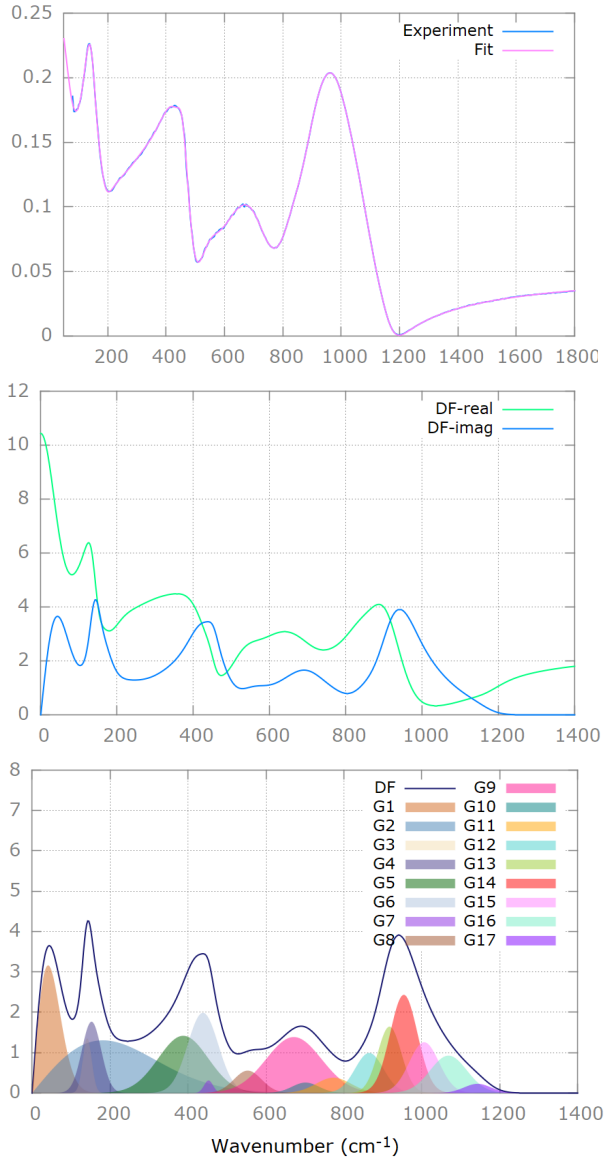

$ZnAl_2Si_2O_8$ glass

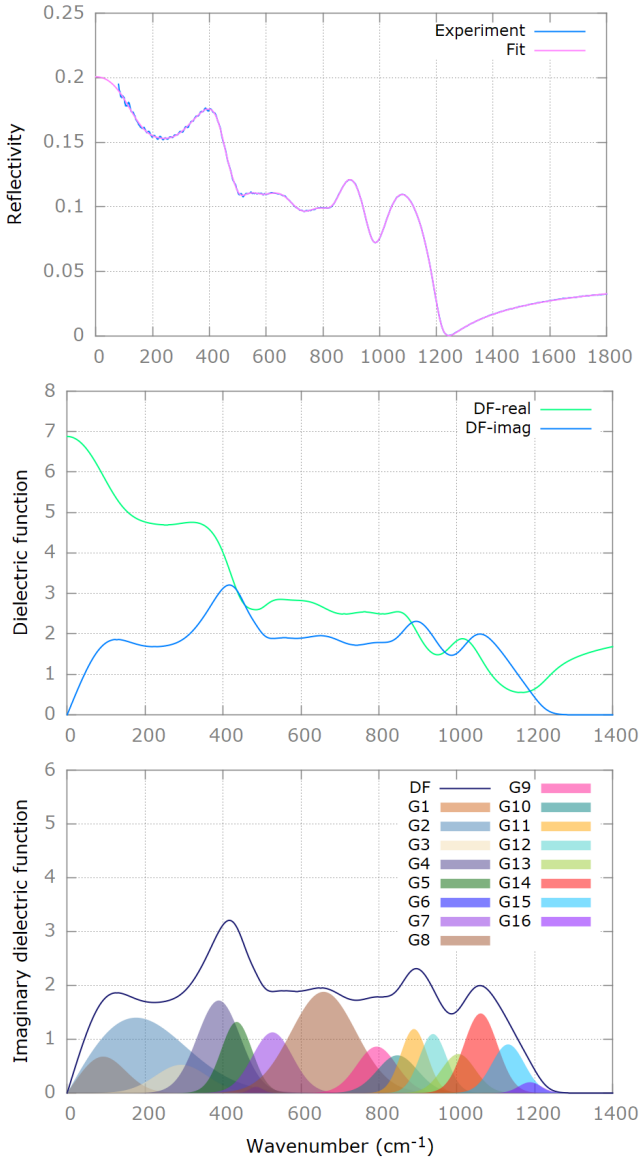

Infrared response of aluminosilicate glasses

Crystal structure of gehlenite

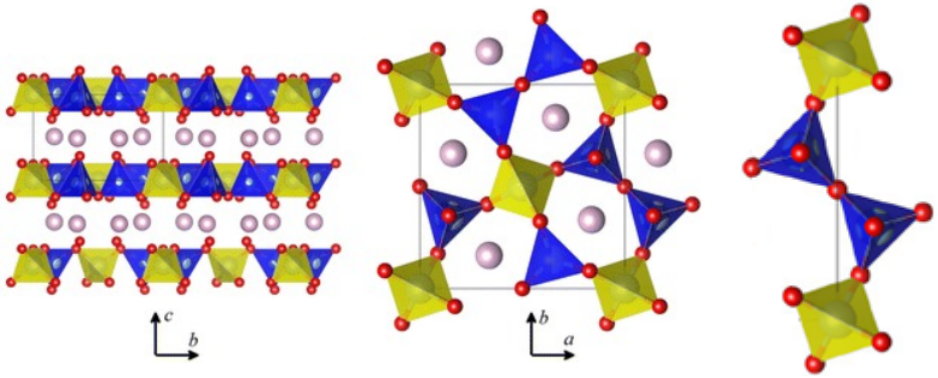

Yellow tetrahedra : Wyckoff site 2a labelled T_1 is fully occupied by Al atoms

AlO_4

Blue tetrahedra : Wyckoff site 4e, labelled T_2 is filled with a mix of Al (50 %) and Si (50 %) atoms

AlO_4 100% Q_3^{3Al}

$Ca_2Al_2SiO_7$ glass

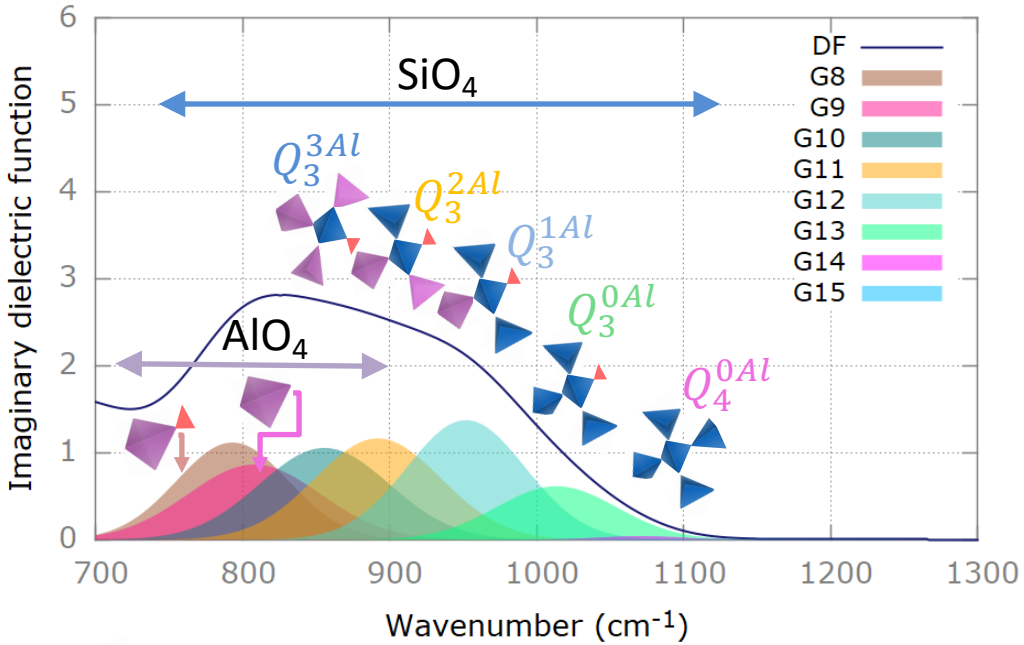

AlO_4

AlO_4 with a non bridging oxygen

Q_n^{mAl} *structural units*

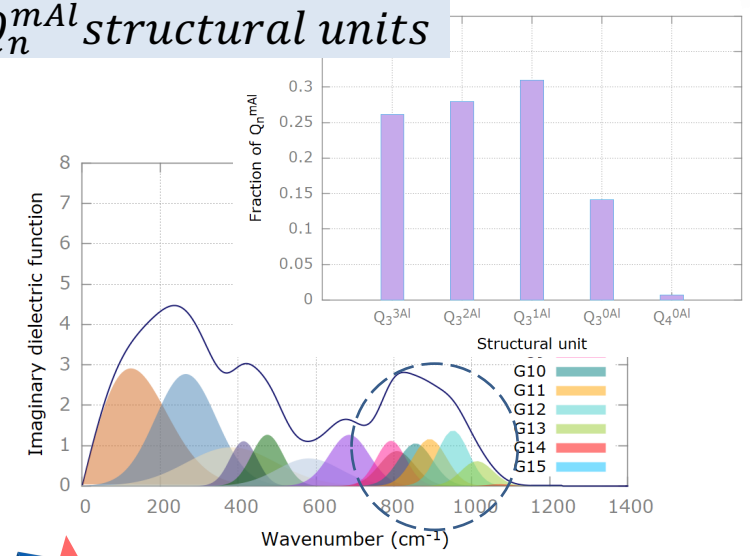

SiO_4 with a non bridging oxygen

Access to structural information

Q_n^{mAl} structural units

Nature of AlO_4 tetrahedra

Infrared response of aluminosilicate glasses

Crystal structure of $BaAl_2Si_2O_8$ (paracelsian)

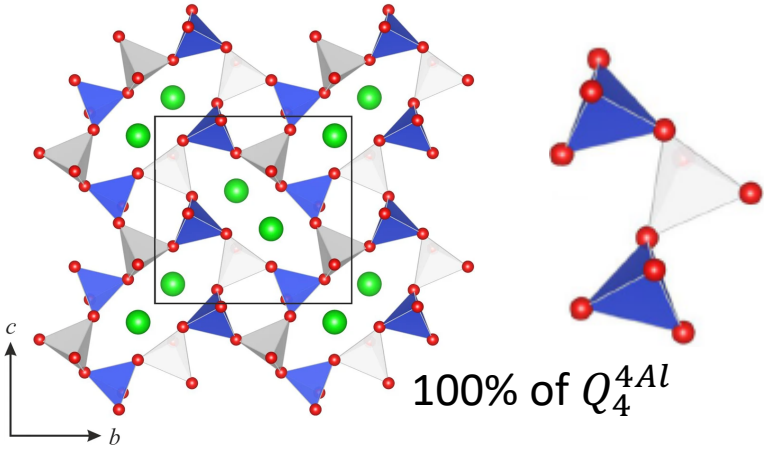

100% of Q_4^{4Al}

Blue tetrahedra : Al atoms (AlO_4) surrounded by 4 Al atoms.

Gray tetrahedra : Si atoms (SiO_4) surrounded by 4 Al atoms.

$BaAl_2Si_2O_8$ glass

Q_n^{mAl} *structural units*

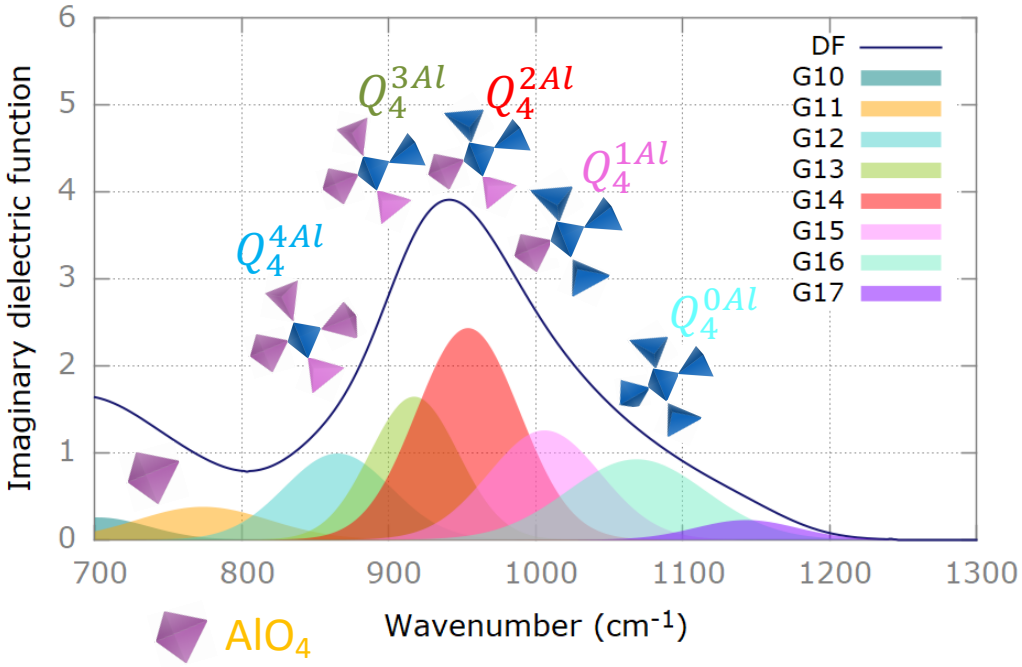

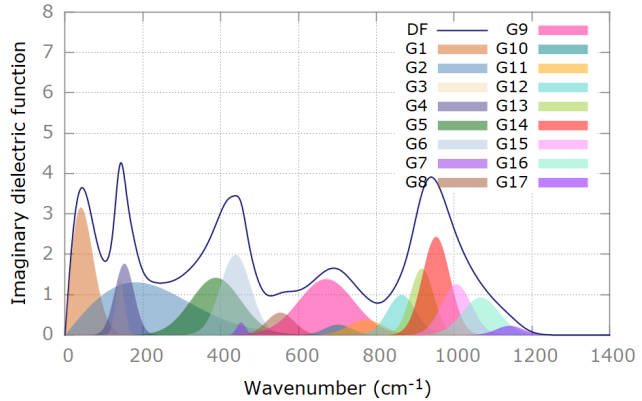

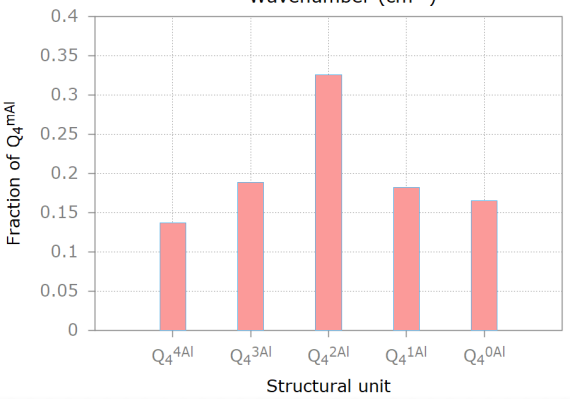

Broad distribution of Q_4^{mAl} structural units.
Al-O-Al bonds

Infrared response of aluminosilicate glasses

$ZnAl_2Si_2O_8$ glass

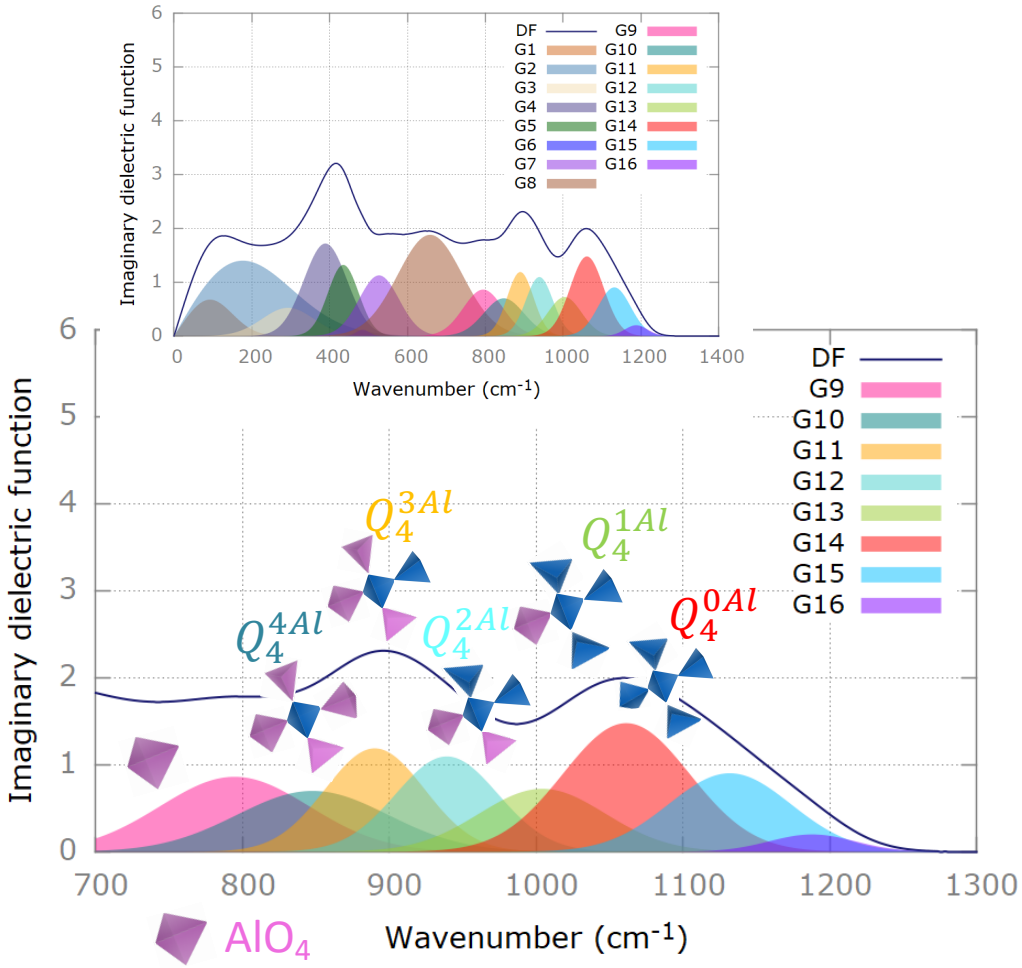

Asymmetric distribution of Q_4^{mAl} structural units for $ZnAl_2Si_2O_8$.

Q_n^{mAl} *structural units*

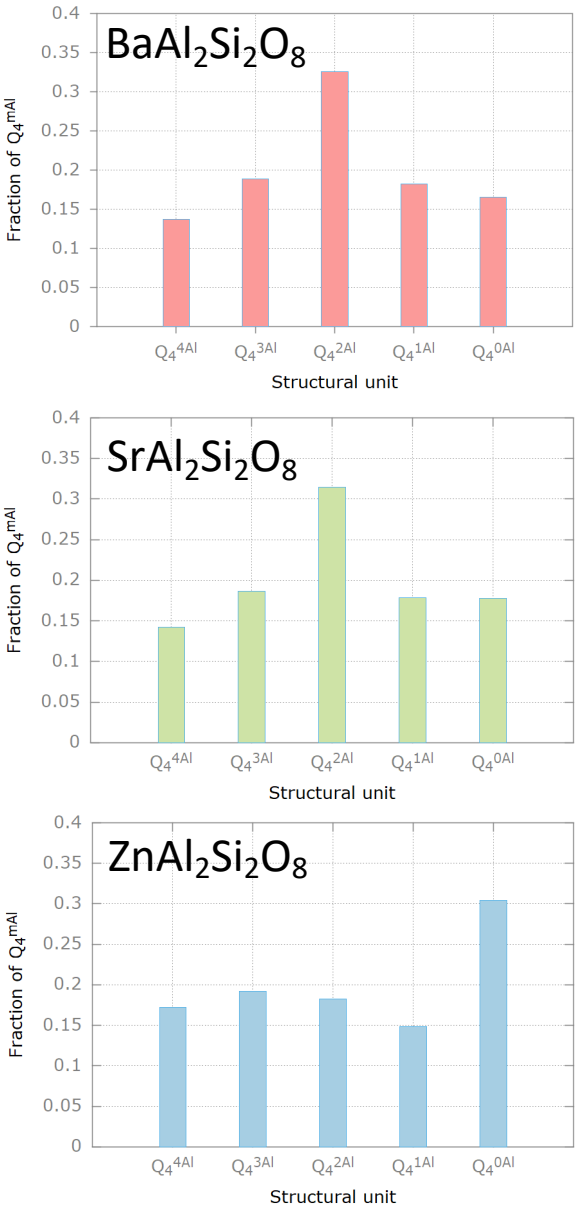

Infrared response of aluminosilicate glasses

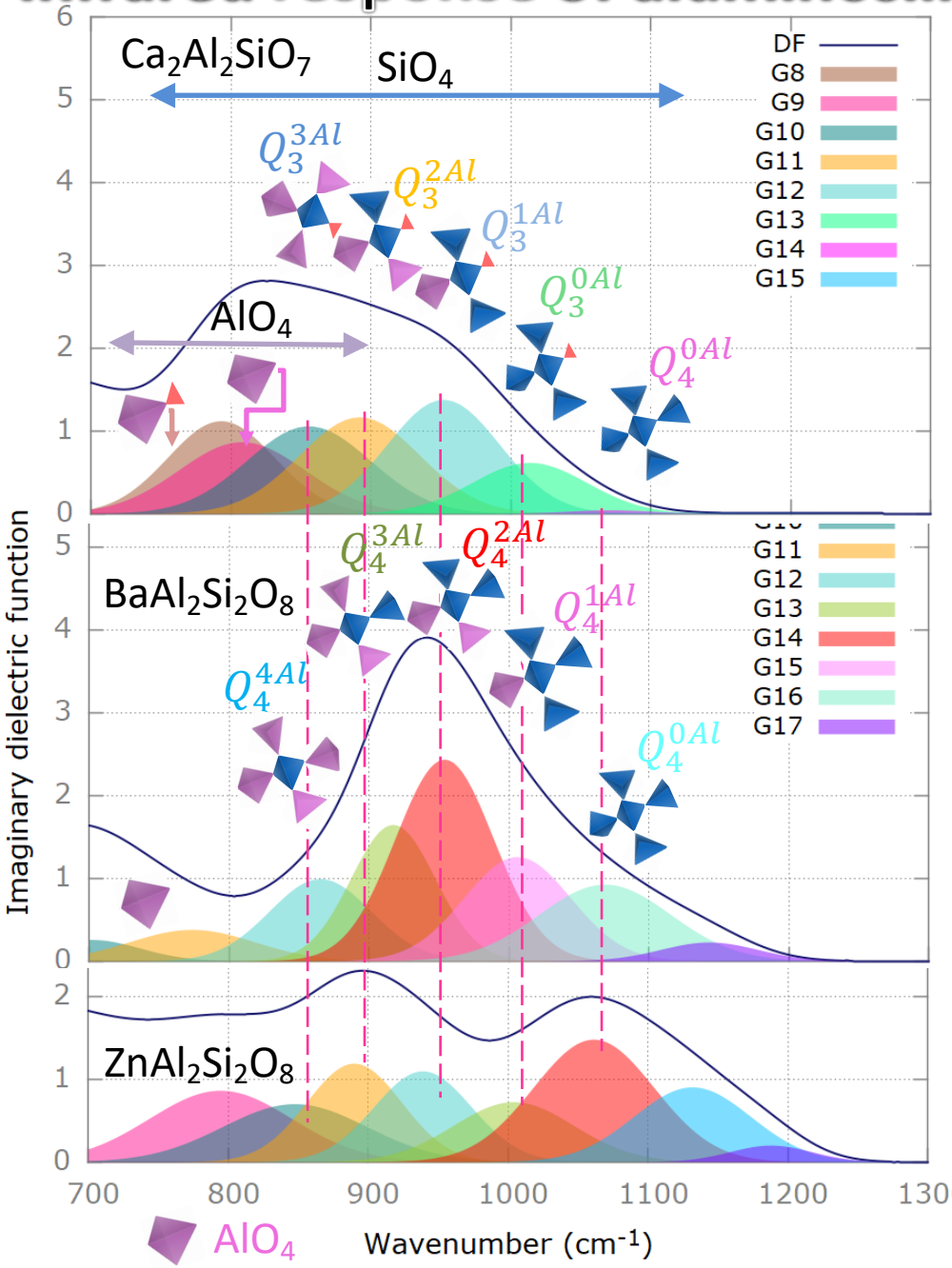

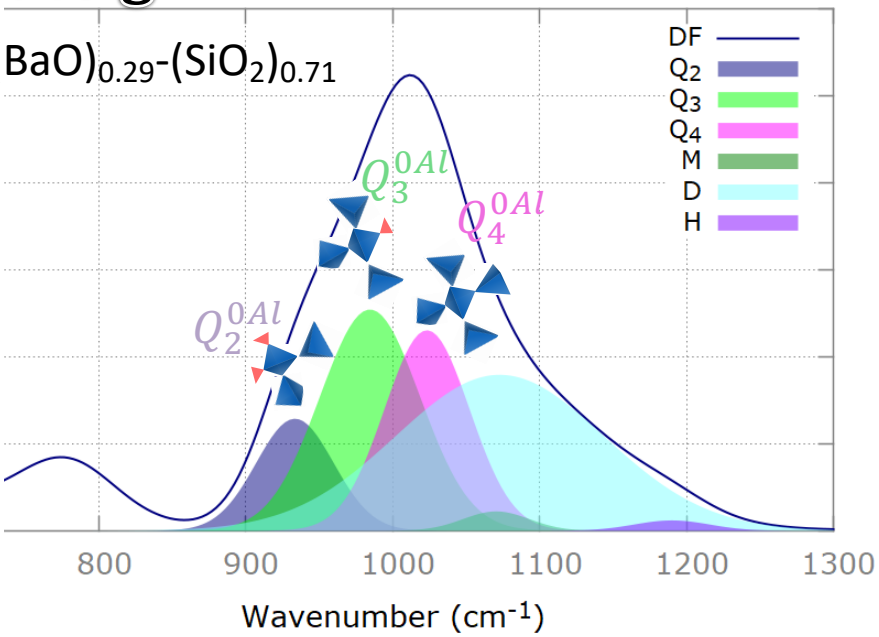

Q_n^{mAl} *structural units*

Absorption band position (cm^{-1})

≅ 860	≅ 900	≅ 950	≅ 1010	≅ 1060
Q_4^{4Al}	Q_4^{3Al}	Q_4^{2Al}	Q_4^{1Al}	Q_4^{0Al}
Q_3^{3Al}	Q_3^{2Al}	Q_3^{1Al}	Q_3^{0Al}	
		Q_2^{0Al}		

Silicate glass containing iron

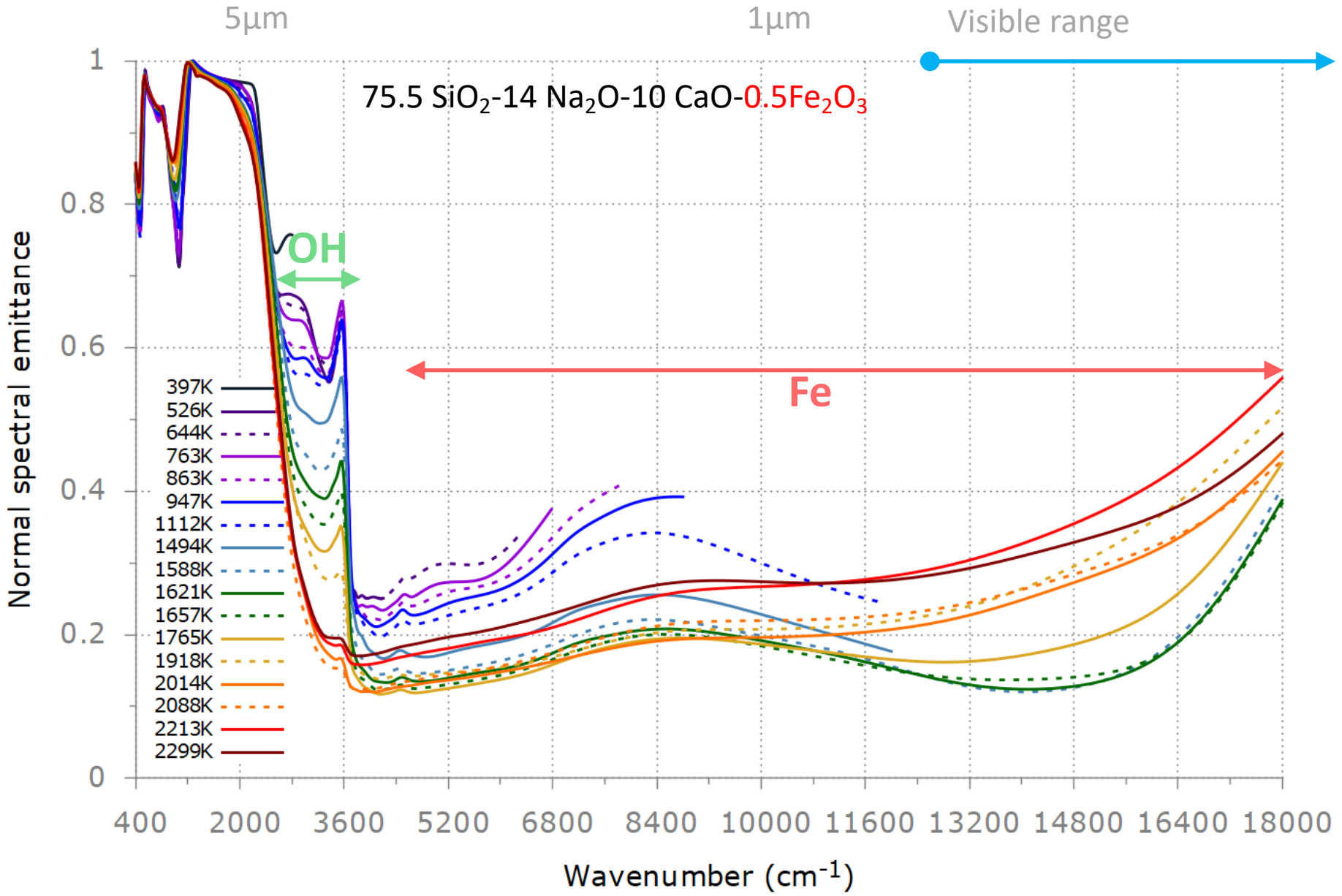

Silicate glass containing iron

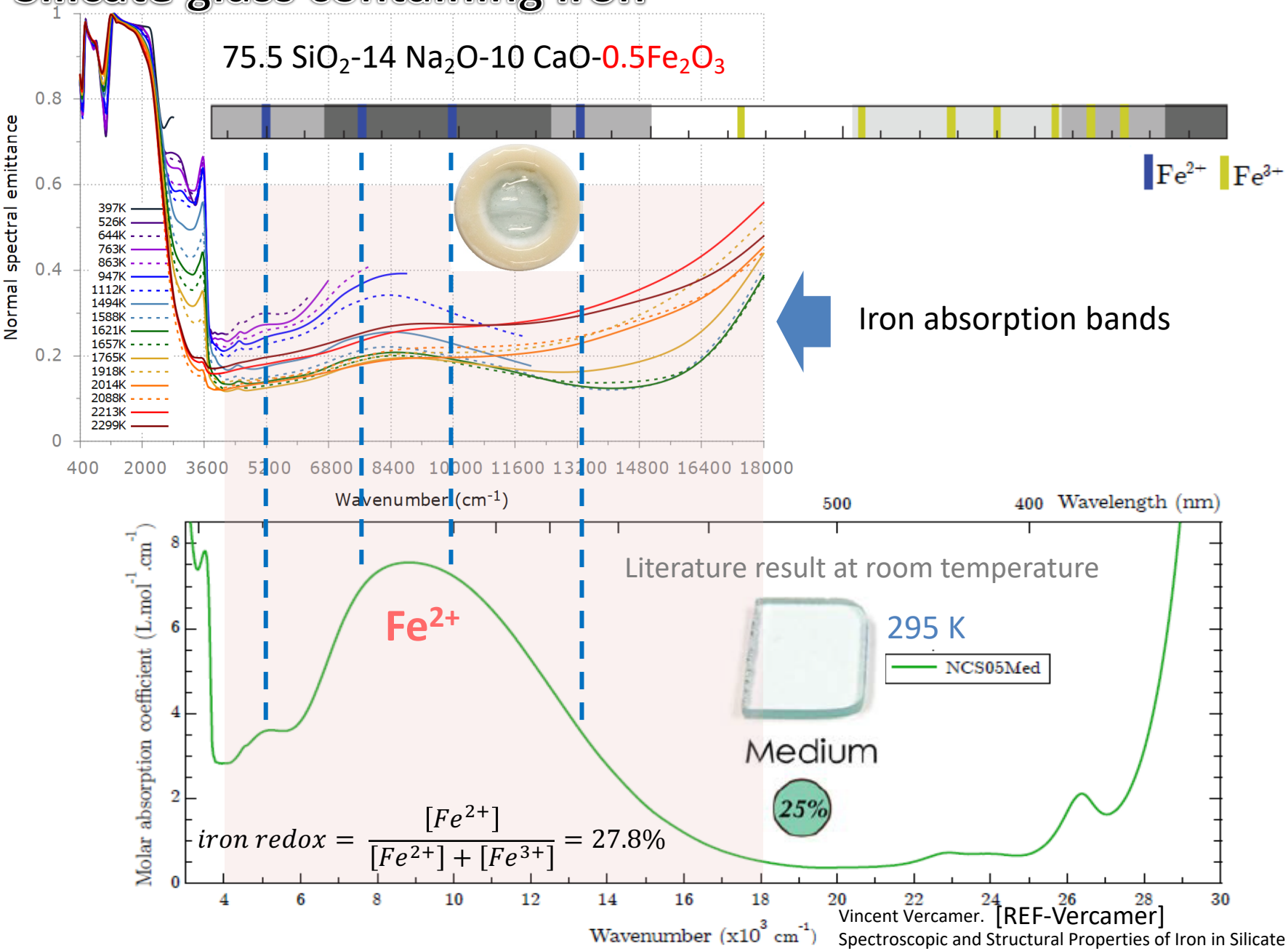

Vincent Vercamer. [REF-Vercamer]
Spectroscopic and Structural Properties of Iron in Silicate Glasses. Material chemistry. Université Pierre et Marie Curie - Paris VI, 2016

Silicate glasses containing iron

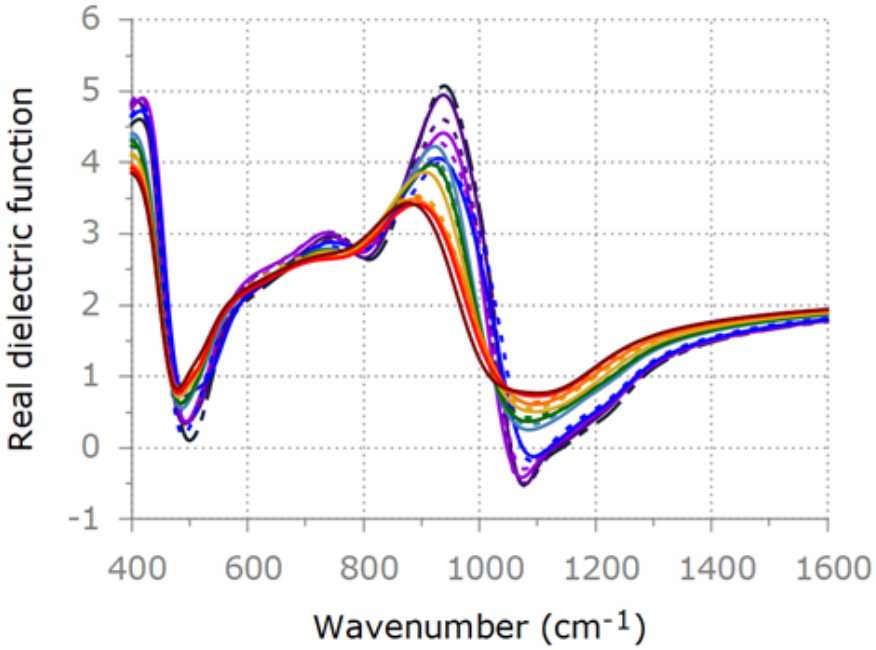

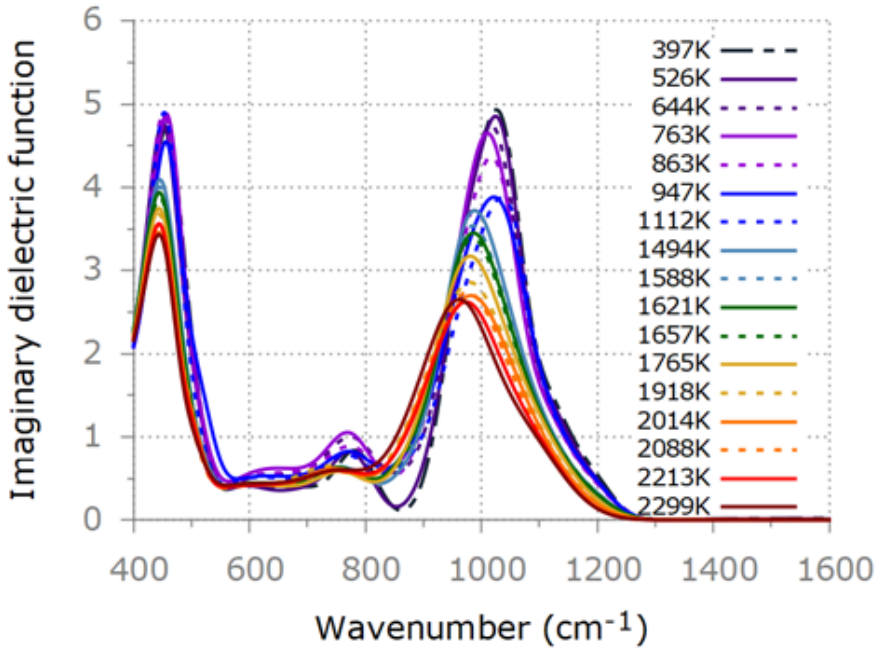

75.5 SiO_2-14 Na_2O-10 CaO-0.5Fe_2O_3

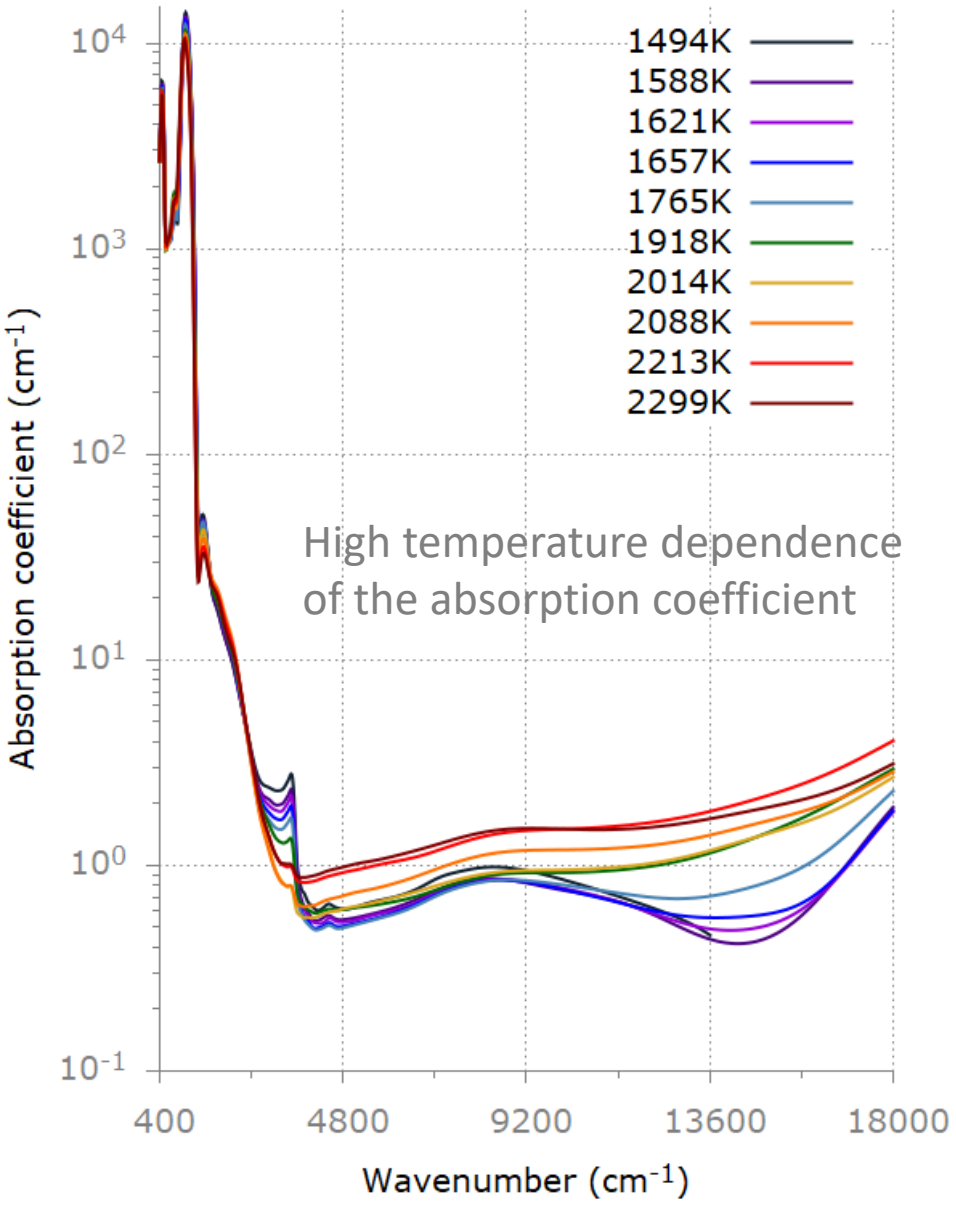

High temperature dependence of the absorption coefficient

Silicate glasses containing iron

75.5 SiO_2-14 Na_2O-10 CaO-0.5Fe_2O_3

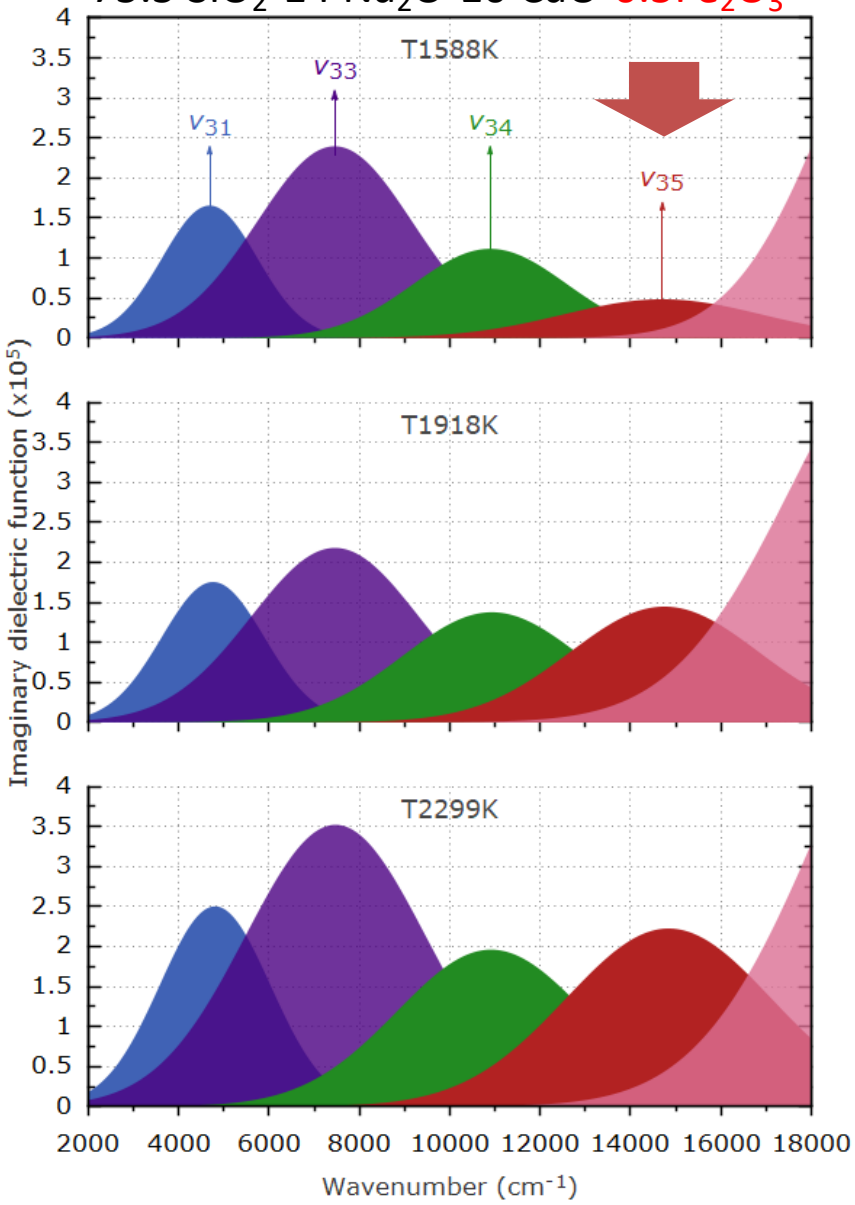

Fit of Fe^{2+} bands with 3 Gaussian functions for NCS05Red [REF-Vercamer]

	Position (cm^{-1})	σ (cm^{-1})	FWHM (cm^{-1})	Intensity (cm^{-1})	$\varepsilon_{Fe^{2+}}$ (L/mol/cm)	Area (cm^{-2})
NCS05Red fit3						
#1	4848	492	1159	0.75	4.8	651.6
#2	7812	1277	3007	0.96	6.2	2181.4
#3	9775	3177	7482	3.65	23.7	20557.5

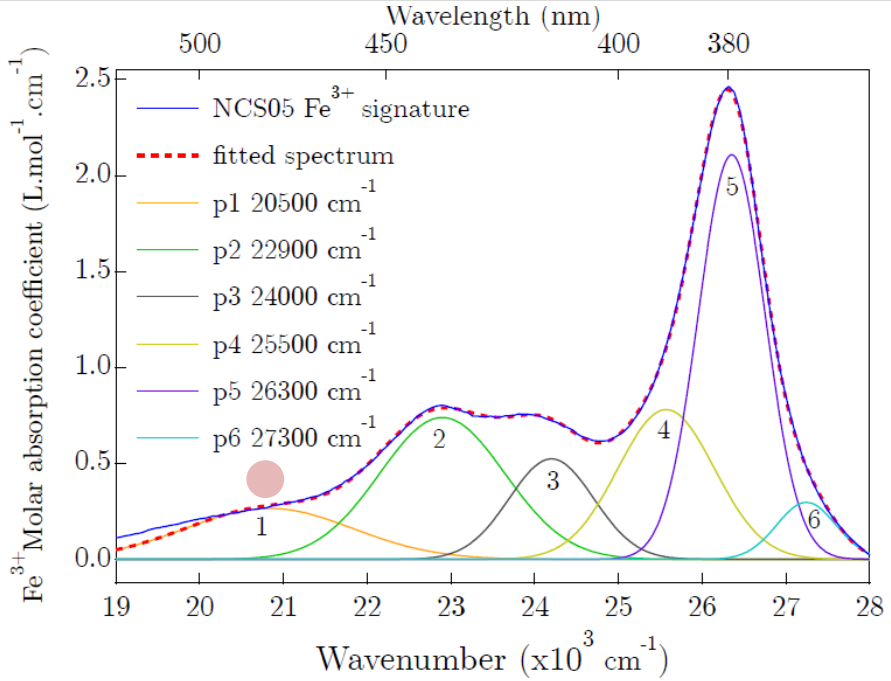

Figure 5.15 – Molar absorption coefficient of Fe^{3+} in the soda-lime oxidized glass (NCS05Ox) after UV-edge removal. Example of Fe^{3+} bands fitted with 6 Gaussians.

Intervalence Charge Transfer (IVCT)

Transfer of an electron between two adjacent Fe^{2+}-Fe^{3+} ions.

Strong increase at high temperature in the melt

Silicate glasses containing iron

75.5 SiO_2-14 Na_2O-10 CaO-0.5Fe_2O_3

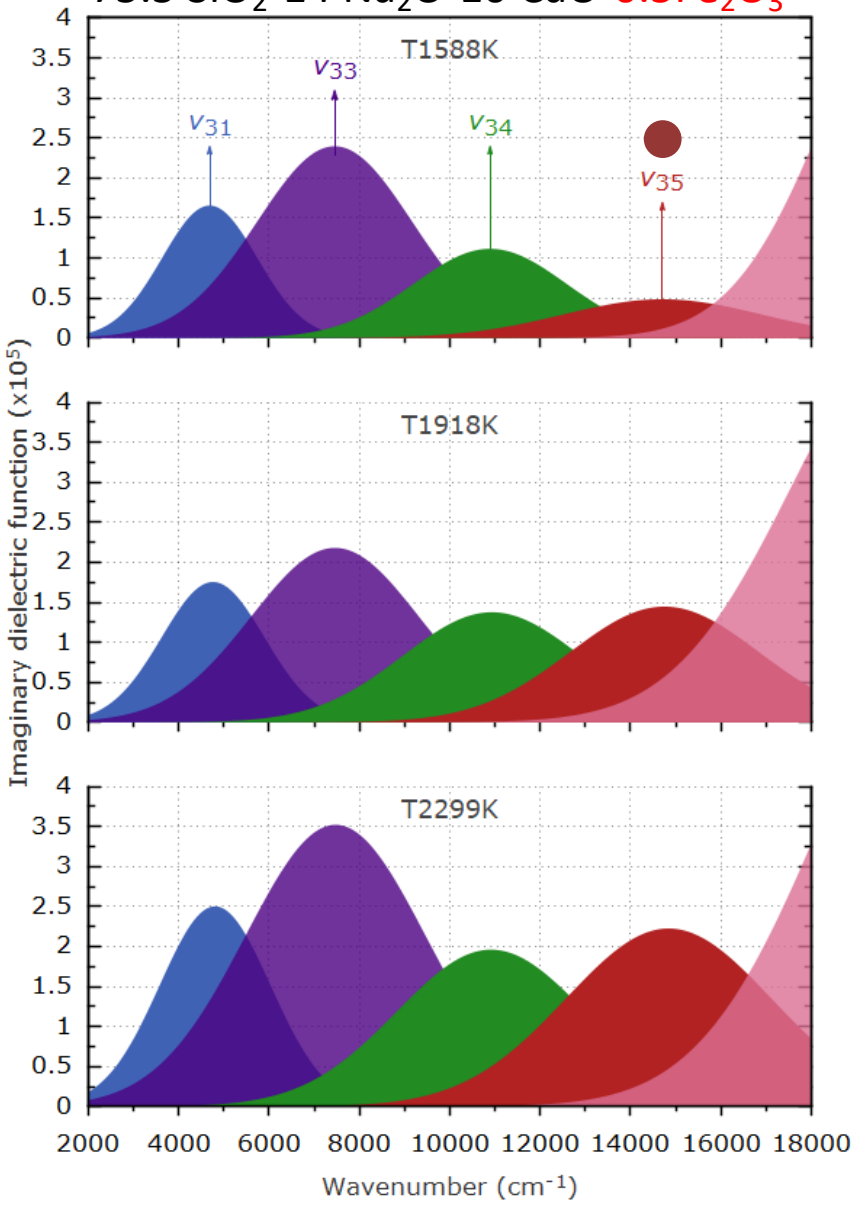

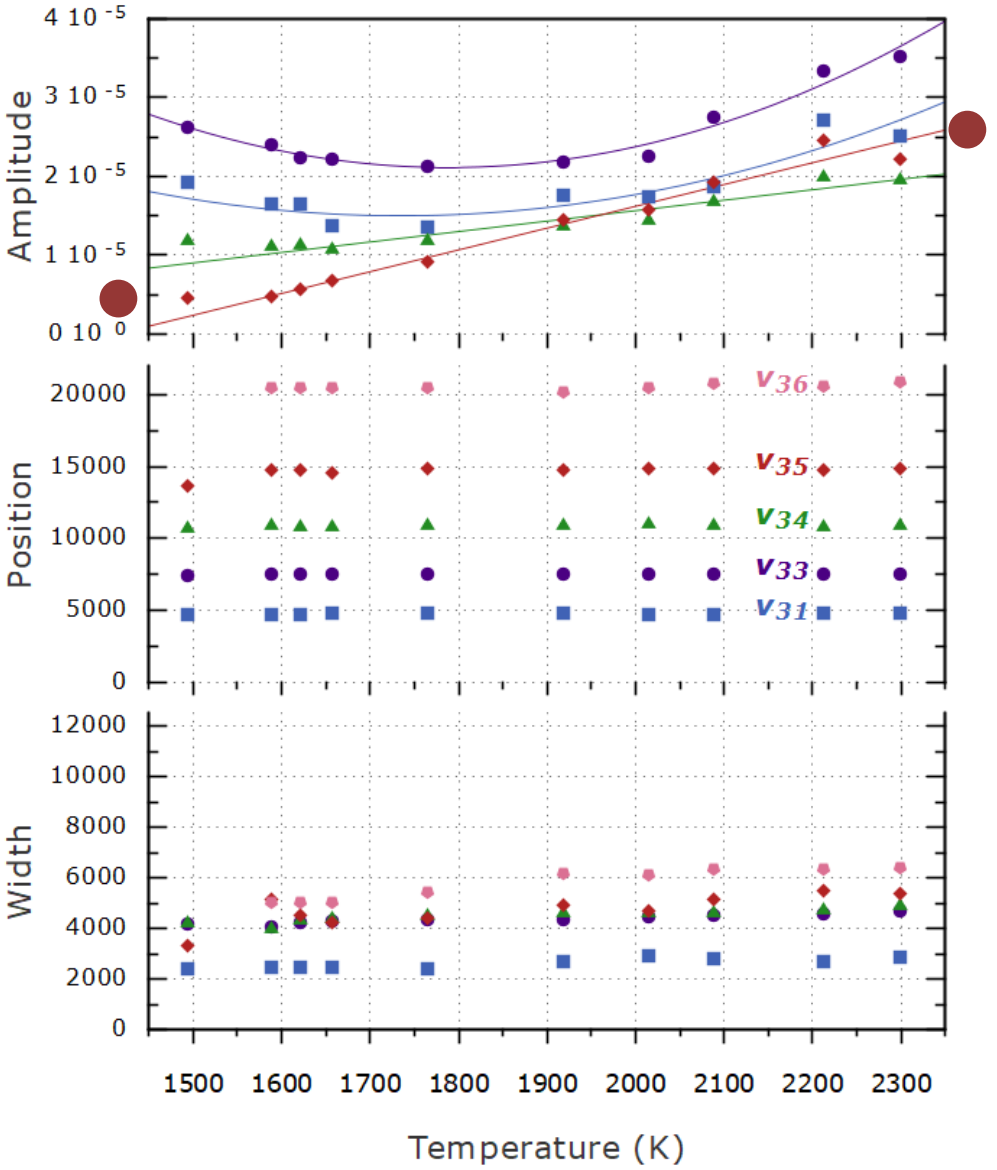

Conclusion

Infrared spectroscopy is a powerful tool to investigate the structural and optical properties of glasses and melts at high temperature.

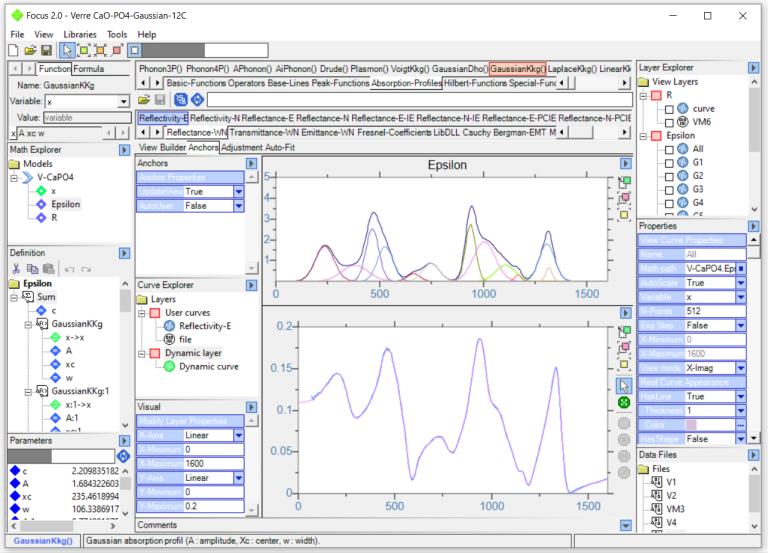

Infrared spectroscopy practical

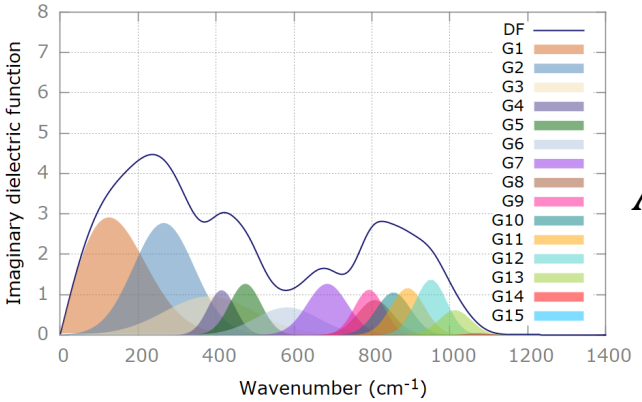

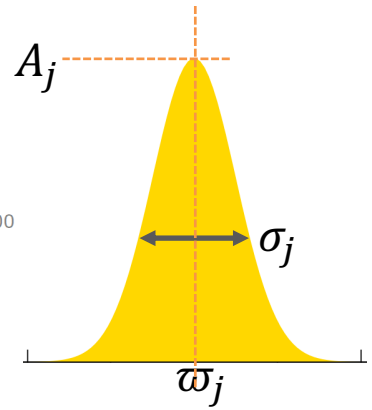

Thank you for your attention

UNION POUR LA SCIENCE ET LA TECHNOLOGIE VERRIÈRES

cnrs Cemhti

POLYTECH ORLÉANS

UNIVERSITE D'ORLEANS